MODELING AND ANALYSIS OF RAIL - WHEEL - FLAT INTERACTION DYNAMICS

By

ARVIND KUMAR GUPTA

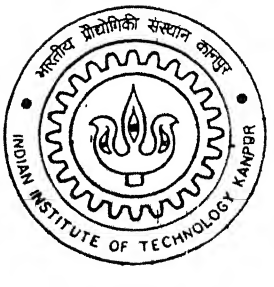

DEPARTMENT OF MECHANICAL ENGINEERING

Indian Institute of Technology Kanpur

FEBRUARY, 2002

MODELING AND ANALYSIS OF RAIL - WHEEL - FLAT INTERACTION DYNAMICS

A Thesis Submitted
in Partial Fulfillment of the Requirements
for the Degree of

MASTER OF TECHNOLOGY

February, 2002

by

ARVIND KUMAR GUPTA

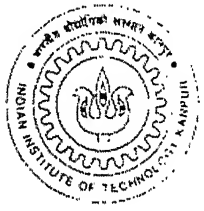

DEPARTMENT OF MECHANICAL ENGINEERING
INDIAN INSTITUTE OF TECHNOLOGY
KANPUR – 208016 (INDIA)

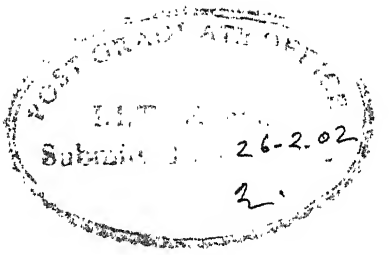

CERTIFICATE

It is certified that the work contained in the thesis entitled "**Modeling and Analysis of Rail - Wheel - Flat Interaction Dynamics**" by ***Arvind Kumar Gupta*** has been carried out under my supervision and that this work has not been submitted elsewhere for a degree.

Dr. Nalinaksh S Vyas
(Professor)
Department of Mechanical Engineering,
Indian Institute of Technology, Kanpur.

February, 2002

ABSTRACT

Development of flats on the wheels of railway engines and wagons is one of the major causes of track and ride quality deterioration. Wheel flats are flat zones on the wheel tread caused by unintentional sliding of the wheel on the rail when the brakes lock. A fresh wheel-flat has the shape of a geometric chord at the wheel circumference. Forces from the wheels with flats can be up to four times higher than those from normal wheels. The objective of the present work is to model the wheel-flat and rail interaction dynamics through a finite element model, in order to understand experimentally observed response of an instrumented railway track. The procedures are validated for free and forced vibration characteristics through comparison with multi-span continuous beam analytical models. Typical wheel flat loading patterns are generated and response is computed for various cases of rigid and flexible rail supports and damping. Response patterns are also compared with test results from an instrumented track.

ACKNOWLEDGEMENTS

I would like to express my sincere gratitude and thanks to my thesis supervisor Dr. N.S. Vyas for his guidance, invaluable suggestions and constant encouragement. I am also grateful to him for exposing me to the practical aspects of vibration diagnostics.

I am thankful to Prashant for his invaluable help and tips with Matlab, Lt.M. V. Rao and Nivea for helping me in all possible ways, Himanshu and Ankur for the lively work environment they have provided.

I appreciate and extend my sincere thanks to Mr. J.P. Verma for his untiring help in sorting out hardware problems.

I am also thankful to my friends Pankaj, Narm, Kuldeep, Subodh, Gajju, Nitesh, Lohani, Lalit and Durgesh, who made lively environment and made my memorable stay here.

Last, I would like to thanks to my Mama, Mami for giving constant supports at every step and I owes my all success to my family, without their support, I can not be here.

Indian Institute of Technology, Kanpur. Arvind Kumar Gupta

February, 2002.

CONTENTS

NOMENCLATURE

N	Number of spans
l_r	Length of rth span
E	Young modulus
I	Area moment of inertia
A	Cross-section area
ρ	Density
r	Span number
x	Distance from origin of in X-direction
t	Time
w_r	Transverse deflection of rth span.
X_r	Normal function of rth span
ω	Natural frequency
B_1, B_2	Constants
P	Force
a_r, b_r, c_r, d_r	Integration constants
k	A parameter ($k^2 = \omega\sqrt{\frac{\rho A}{EI}}$)
ϕ_r	$\coth kl_r - \cot kl_r$
ψ_r	$\operatorname{cosech} kl_r - \operatorname{cosec} kl_r$
δw	Virtual displacement
μ	Function of time
V_e	Strain energy of bending beam
c	Distance from the left end of first span
V	Velocity of moving load
L	Total length of beams
λ_m	A parameter $\left(\lambda_m{}^2 = \frac{EI\int_0^L X''^2{}_m dx}{\rho A\int_0^L X''^2{}_m dx} \right)$
C_m, D_m	Integration constants

LIST OF FIGURES

LIST OF TABLES

CHAPTER 1

INTRODUCTION

Heavier trains and higher speeds accentuate the detrimental influence of imperfections in vehicles and tracks on the dynamic interaction between the two. Large dynamic load may be excited causing significant damage to both track and vehicle. Common imperfections are irregularities on the running surface of rail and wheel and deficiency in the support of track structure. Isolated defects such as wheel flats or badly aligned rail joints result in high frequency vibration, while for example loss of ballast under a single sleeper mostly affects the low frequency response of the track. The dominating frequency excited by a periodic irregularity, such as a sinusoidal corrugation of the railhead or the wheel tread, depends on the wavelength of the irregularity and the speed of train.

The influence of out of roundness of a wheel on the dynamic train/track is often considerable. A severe type of out of roundness is the wheel flat, which is a flat zone on the wheel tread caused by unintentional sliding of the wheel on the rail when the brake locks. A fresh wheel-flat has the shape of a geometric chord at the wheel circumference. However, when the brake unlocks the corners of the flat profile soon become rounded. The forces from the wheel flats are considered to be the decisive contributory factor affecting track degradation and life. Wheel forces primarily influence the rails and concrete sleepers. However, it is known that forces pass through the entire substructure down to the subsoil.

The objective of the present work is to model, the wheel-flat and rail interaction dynamics through a finite element model, in order to understand experimentally observed response of an instrumented railway track. The finite element model is developed using commercially available software (NISA). The finite element procedures are validated for free and forced vibration characteristics through comparison with multi-span continuous beam analytical models. Typical wheel flat loading patterns are generated and response is

computed for various cases of rigid and flexible rail supports and damping. Response patterns are also compared with test results from an instrumented track.

The general problem on rail-wheel interaction attracted attention as early as 1847, when a British commission was appointed to study dynamic effects in railway bridges. The differential equation of deflection was established by neglecting inertia of the bridge and by considering the moving load as a concentrated mass. An exact solution of the equation was obtained by Stokes (1849). The next step was made by Timeshenko (1922), who solved the problem of a pulsating forces moving with uniform velocity along a beam. Other work has been done, including that of Lowan (1935), who studied the case in which the velocity of traversing force is not constant. The foregoing investigations were all limited to single span structures. After that Ayre, Ford, and Jacobsen (1950) have studied transverse vibration of a two - span beam under action of a moving constant force. Some of the more recent works include work done by Cai, Cheung and Chan (1988) who studied dynamic response of infinite continuous beam subjected to moving force. They made the assumption that slope and moment at right end of last span is equal to slope and moment at left end of first span respectively. For multi-span beams most researchers have used Finite Element methods. Nielsen and Igeland (1995) has investigated vertical dynamic behaviour for a railway bogie moving on a rail by use of an extended state-space vector approach in conjunction with a complex modal superposition for the track. Effects of imperfections on the running surface of wheel and rail were studied by assigning irregularity function to these surface and calculated contact forces for moderate vehicle speed in the presence of wheel flat. Thambiratnam and Zhuge (1996) have developed simple finite element model to analyze simply supported beams on an elastic foundation of any length, where the foundation has been modeled by springs of variable stiffness. The effect of the speed of moving load, foundation stiffness and length of beam on the response of the beam have been studied and dynamic amplification of deflection and stress have been evaluated. Abu Hilal and Zibdeh (2000) have investigated vibration of elastic homogeneous isotropic beam with general boundary condition traversed by moving force. They however, considered only single span beams. Wu and Shih (2000) have studied dynamic response of railway and carriage under the

high speed moving loads. Dynamic response of the rail and carriage due to action of multi-roller carriage was determined by means of the finite element method. Wu, and Thompson (2001) have investigated vibration analysis of railway track with multiple wheel on the rail. However the focus is on railway rolling noise.

A wheel flat is caused by the brake or some other mechanism, interfering with the normal angular velocity of the wheel. When brakes do not function properly, the wheel ceases to rotate and a flat develops due to plastic deformation. The dimensions of the wheel flat, its form and position on the tread depends on length of the wheel skid, axle loading, running speed, shape of rail profile, position of the wheel on rail, wheel material and the material coefficient of adhesion between the wheel and the rail material.

Wheel flats cause large dynamic forces to the track. According to popular practices, flats on wheels should be restricted to a length of 60 mm and a depth of 0.9-1.4 mm. In this range dynamic wheel load increases by approximately 30 kN/mm for timber sleepers and 50 kN/mm for concrete sleepers. Wheel flats are also known to cause very high acceleration (approx. 500 g) on the track. These high acceleration become input to the rolling stock, which will induce greater forces than permitted and damage the suspension system frame and the body of the rolling stock. These forces may also cause bearing damage and hot axles boxes. Wheel with flats causes local unevenness on the tread. The foreign bodies may penetrate in to the tread due to wheel deformation. Deformed wheels are also damaged by the heavy impacts. In addition, excessive vibration and unpleasant air borne noise is caused which is irritating to the passengers.

In the present work the rail track has been modeled as a multi-span continuous beam with rigid or flexible supports at regular intervals. The free vibration analytical model is described in Chapter 2 along with the finite element model. Forced vibration under a single moving load is discussed in Chapter 3 and the finite element procedure is validated by comparison with results from an analytical solution. Rail response under a moving train, with representative data, is obtained from the finite element model in Chapter 4, for cases of wheel with flat and without flat. The results are compared with those from a test site. Conclusions and scope for future work are given in Chapter 5.

CHAPTER 2

FREE VIBRATIONS OF MULTI-SPAN CONTINUOUS BEAMS

Mathematical models of varying degrees of complexity have been developed by researchers to analyze rail-wheel interaction. The focus of the present study is to develop a Finite Element model of the rail in order to study its response under typical wheel-flat loading. The free-vibration characteristics of rails are functions of its geometric and material characteristics. It is customary to model the rail as a continuous beam with multiple supports. These supports to the rail come in the form of wooden or concrete sleepers, which are laid out periodically across the rail (Fig.2.1). The sleepers can be modeled as rigid supports or flexible springs. Free vibration characteristics of rails modeled as multi-span continuous beams are discussed in this chapter. The analytical formulation is based on the procedure suggested by Timoshenko (1955) and is employed to validate the results from the finite element model.

2.1 Governing Equation

Consider the case of a continuous Euler - Bernoulli beam with N spans simply supported at the ends and (N-1) intermediate support. Let $l_1, l_2, \ldots\ldots l_N$ be the lengths of consecutive spans, the flexural rigidity of the beam being the same for all spans. Taking the origin of coordinates at the left end of each span as shown in Fig. 2.2,

the equation for transverse vibration for each span is given by

$$EI \frac{\partial^4 w_r}{\partial x_r^4} + \rho A \frac{\partial^2 w_r}{\partial t^2} = 0, \qquad 0 \le x_r \le l_r, \qquad r = 1,2.,\ldots\ldots N \tag{2.1}$$

Suffix r denotes the rth span, EI, ρ and A denote, respectively, the flexural rigidity, mass density and the cross-sectional area. w is the transverse deflection of each span, x is the local coordinate along the axis of the rth span and t is the time . The continuity and equilibrium condition at the intermediate support points of the continuous beam require following relations:

$$w_r(x_r = 0, t) = 0,$$

$$w_r(x_r = l_r, t) = 0,$$

$$\frac{\partial w_r}{\partial x_r}(x_r = l_r, t) = \frac{\partial w_{r+1}}{\partial x_{r+1}}(x_{r+1,} = 0, t),$$

$$\frac{\partial^2 w_r}{\partial x_r^2}(x_r = l_r, t) = \frac{\partial^2 w_{r+1}}{\partial x^2_{r+1}}(x_{r+1} = 0, t), \qquad r=1,2,\ldots\ldots N\text{-}1 \qquad (2.2)$$

2.2 Response

Let the solution of equation (2.1) be given by

$$w_r = X_r(x) * (B_1 \sin \omega t + B_2 \cos \omega t) \qquad (2.3)$$

where X_r is normal function for span r and ω is the natural frequency and B_1 and B_2 are constants.

The normal function for the span r will be

$$X_r = a_r \cos kx + b_r \cosh kx + c_r \sin kx + d_r \sinh kx \qquad (2.4)$$

Substitution of the first of boundary conditions given in (2.2) gives

$a_r = - b_r,$

so that

$$X_r = a_r(\cos kx - \cosh kx) + c_r \sin kx + d_r \sinh kx \qquad (2.5)$$

In the above a_r, c_r, d_r remain constants to be determined from the condition at the ends of the span and

$$k^2 = \omega\sqrt{\frac{\rho A}{EI}} \qquad (2.6)$$

The consecutive derivatives of (2.4) will be

$$X'_r = a_r k(\sin kx + \sinh kx) + c_r k \cos kx + d_r k \cosh kx \qquad (2.7)$$

$$X''_r = -a_r k^2(\cos kx + \cosh kx) - c_r k^2 \sin kx + d_r k^2 \sinh kx \qquad (2.8)$$

From the condition at the simply supported ends of the beam it can now be concluded that

$a_1 = a_{N+1} = 0.$

Considering the condition at the right end of span r we have,

$$(X_r)_{x=l_r} = 0,$$

$$(X'_r)_{x=l_r} = (X'_{r+1})_{x=0},$$

$$(X''_r)_{x=l_r} = (X''_{r+1})_{x=0}, \qquad (2.9)$$

Now from equations. (2.4), (2.7), (2.8) one gets

$$a_r(\cos kl_r - \cosh kl_r) + c_r \sin kl_r + d_r \sinh kl_r = 0, \qquad (2.10)$$

$$-a_r(\sin kl_r + \sinh kl_r) + c_r \cos kl_r + d_r \cosh kl_r = c_{r+1} + d_{r+1}, \qquad (2.11)$$

$$a_r(\cos kl_r + \cosh kl_r) + c_r \sin kl_r - d_r \sinh kl_r = 2a_{r+1}, \qquad (2.12)$$

Equations (2.10) - (2.12) can be solved to obtain

$$c_r = \frac{a_{r+1} - a_r \cos kl_r}{\sin kl_r},$$

$$d_r = \frac{-a_{r+1} + a_r \cosh kl_r}{\sinh kl_r} \qquad \text{(for } \sin kl_r \text{ not zero)} \qquad (2.13)$$

From the above

$$c_r + d_r = a_r(\coth kl_r - \cot kl_r) - a_{r+1}(\operatorname{cosech} kl_r - \operatorname{cosec} kl_r) \qquad (2.14)$$

Using notations:

$$\coth kl_r - \cot kl_r = \phi_r$$

$$\operatorname{cosech} kl_r - \operatorname{cosec} kl_r = \psi_r \qquad (2.15)$$

we obtain

$$c_r + d_r = a_r\phi_r - a_{r+1}\psi_r$$

Similarly, for the span $r+1$,

$$c_{r+1} + d_{r+1} = a_{r+1}\phi_{r+1} - a_{r+2}\psi_{r+1} \qquad \ldots.(2.16)$$

Substituting equations (2.13) and (2.16) in equations. (2.11), we obtain

$$a_r\psi_r - a_{r+1}(\phi_r + \phi_{r+1}) + a_{r+2}\psi_{r+1} = 0 \qquad (2.17)$$

Writing analogous equations for each intermediate support, the following system of (N-1) equations will be obtained:

$$-a_2(\phi_1 + \phi_2) + a_3\psi_2 = 0,$$

$$a_2\psi_2 - a_3(\phi_2 + \phi_3) + a_4\psi_3 = 0,$$

. . . . . .

. . . . . .

$$a_N\psi_{N-1} - a_N(\phi_{N-1} + \phi_N) = 0, \qquad (2.18)$$

The frequency equation for the free vibration will be obtained by putting the determinant of the above equations equal to zero.

If the length of each span is same means $l_1=l_2=l_N=l$ then the relation for first natural frequency is

$$k_1 l = \pi$$

Natural frequency and mode shapes can be found by solving equations (2.18), (2.6) and (2.5).

2.3 Finite Element Model

The analytical formulation described in the previous section is employed to compare the results from a finite element model for a multi-span beam. The finite element algorithm is to be used further to model the rail track. A simple 2-D beam-element, with eight elements per span, has been employed in the finite element model. There are two nodes per element and the element has 3 degrees of freedom namely,

u_x = displacement in X-direction,

u_y = displacement in Y-direction,

r_z = rotation about Z-direction.

u_x = 0 at all nodes and u_y=0 at supports

Two beams with 15 and 25 spans respectively, as shown in in Figs.2.3.(a) and (b) were chosen to carry out the free vibration modeling exercise and comparison of results with the analytical model described in sections 2.1 - 2.2. For Beam 1, with 15 spans the total number of elements was 120 (121 nodes), while for Beam 2, with 25 spans the total number of elements was 200 (201 nodes).

2.4 Numerical Results

The numerical exercise was carried out for the following set of data

Young modulus of beam $E = 2\times10^{11}$ N/m

Cross section Area of beam $A = 9\times10^{-4}$ m^2

Area moment of inertia $I = 6.75\times10^{-8}$ m^4

Density of beam material $\rho = 8000$ Kg/m^3

Length of each span $l = 1$ m

The eigenvalue problem of equations (2.18) is solved to obtain natural frequencies and mode shapes of beams with 15 and 25 spans. Eigenvalue analysis of the beams was carried out in NISA using conventional subspace iteration and consistent mass formulation. First ten natural frequencies thus obtained analytically are given for 15 span and 25 span beams in Table 2.1 and Table 2.2 respectively. The results obtained from the FE model developed using the commercially available software NISA are also given in the tables. The close agreement between the two sets of results validate the finite element modeling procedure in NISA. The corresponding mode shapes for the two beams are shown in Figs. 2.4 (a), (b) and 2.5 (a), (b) respectively.

Table 2.1 Natural frequencies for 15 span beam

Mode No.	Analytical model (rad/s)	FE model (rad/s)
1	427.37	427.22
2	432.81	432.65
3	448.74	448.58
4	474.14	473.97
5	507.62	507.43
6	547.68	547.47
7	592.91	592.68
8	642.01	641.76
9	693.74	693.47
10	746.81	746.51

Table 2.2 Natural frequencies for 25 span beam

Mode No	Analytical model (rad/s)	FE model (rad/s)
1	427.37	427.21
2	429.33	429.18
3	435.18	435.02
4	444.76	444.60
5	457.84	457.67
6	474.14	473.97
7	493.35	493.17
8	515.15	514.96
9	539.21	539.00
10	565.22	565.001

Fig 2.1 Rails supported on sleeper pads

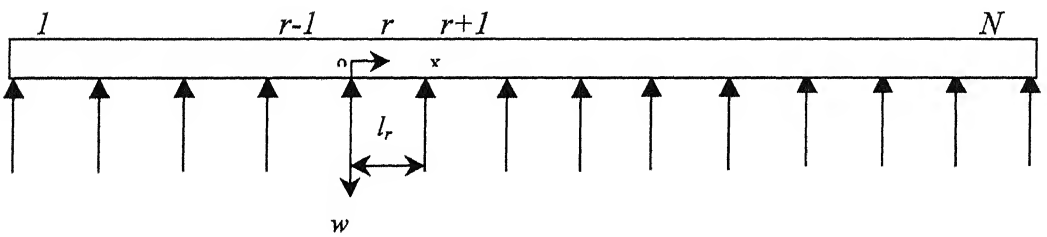

Fig 2.2 Multi-span continuous beam

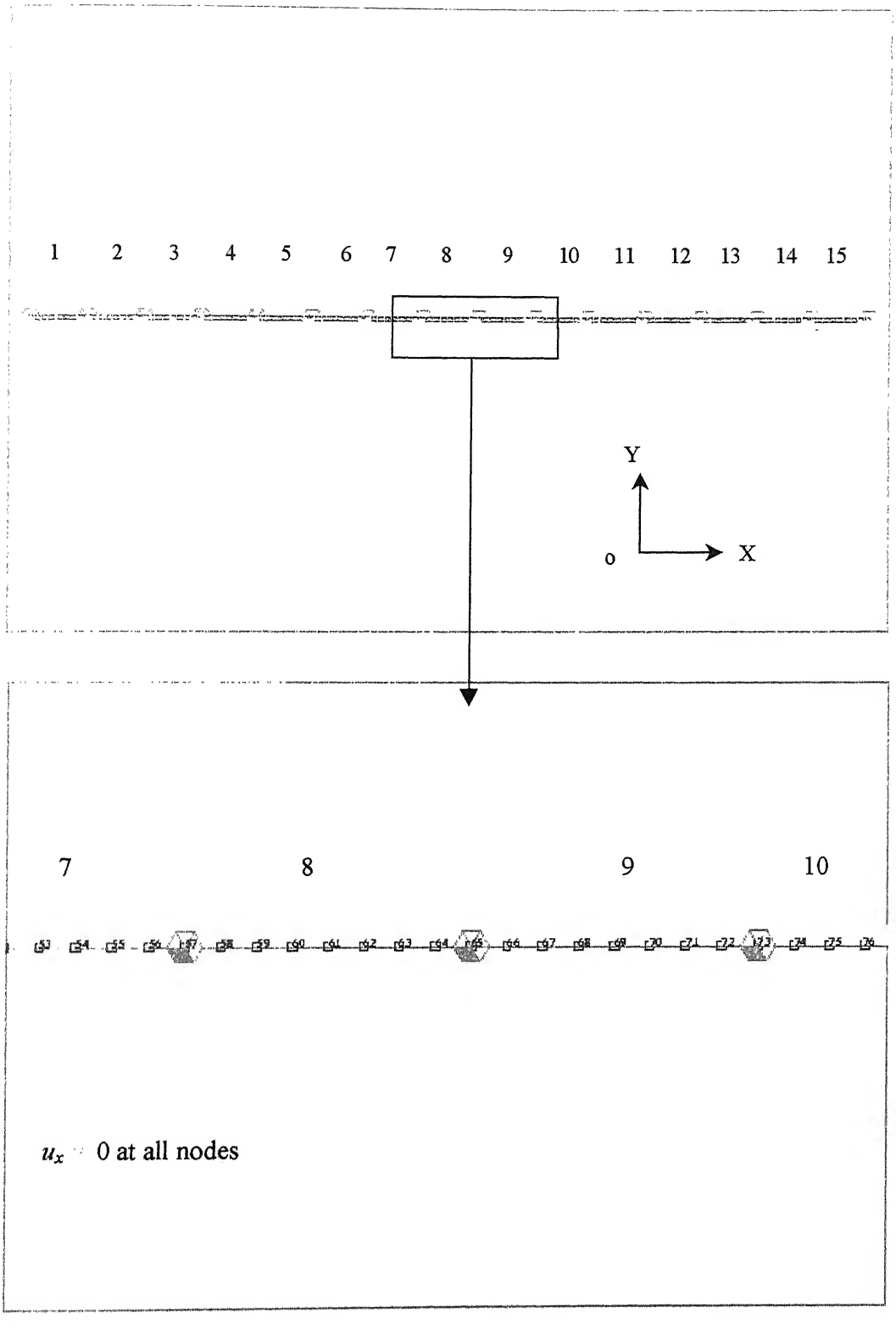

Fig 2.3 (a) Finite element model of 15 span beam

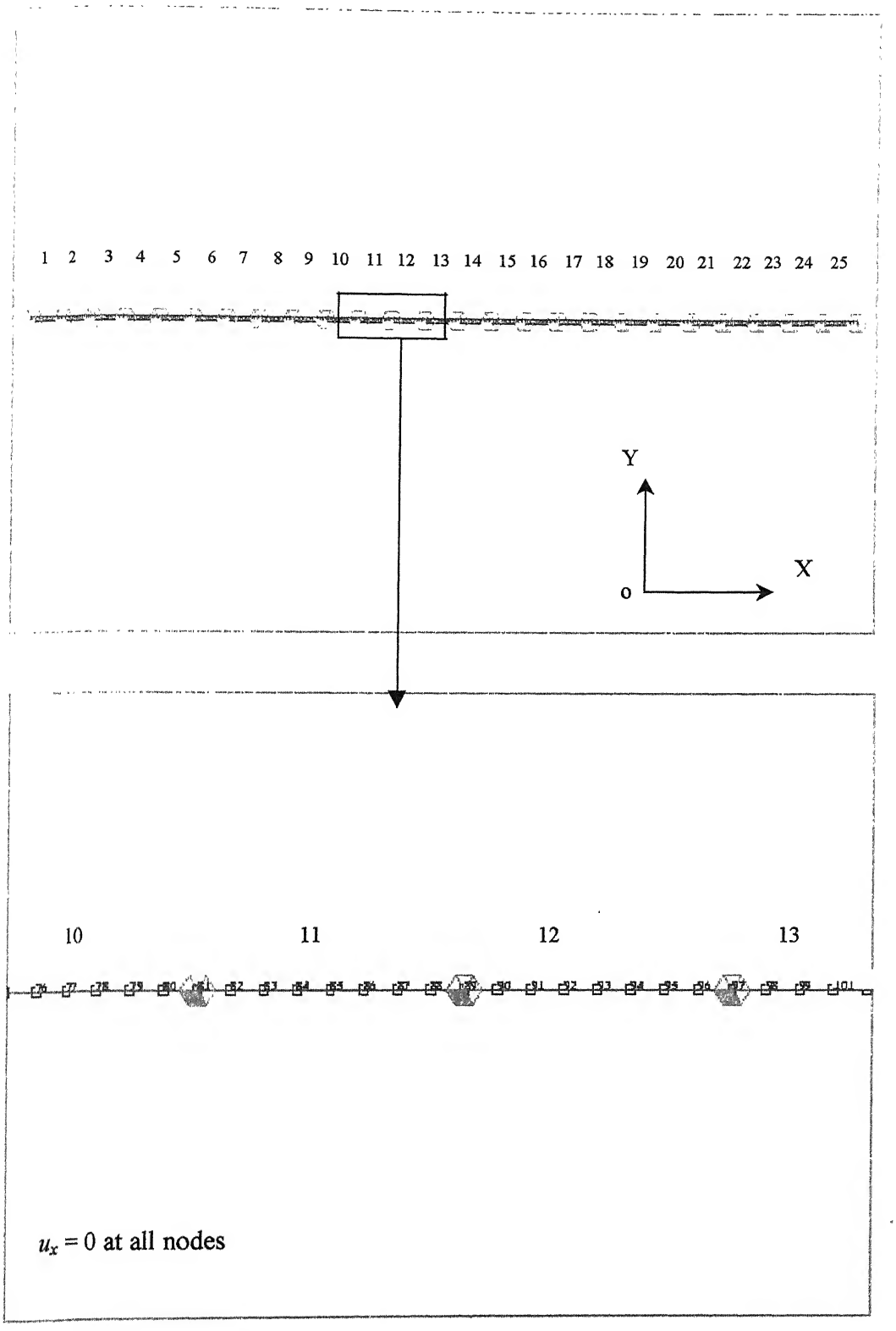

Fig 2.3 (b) Finite element model of 25 span beam

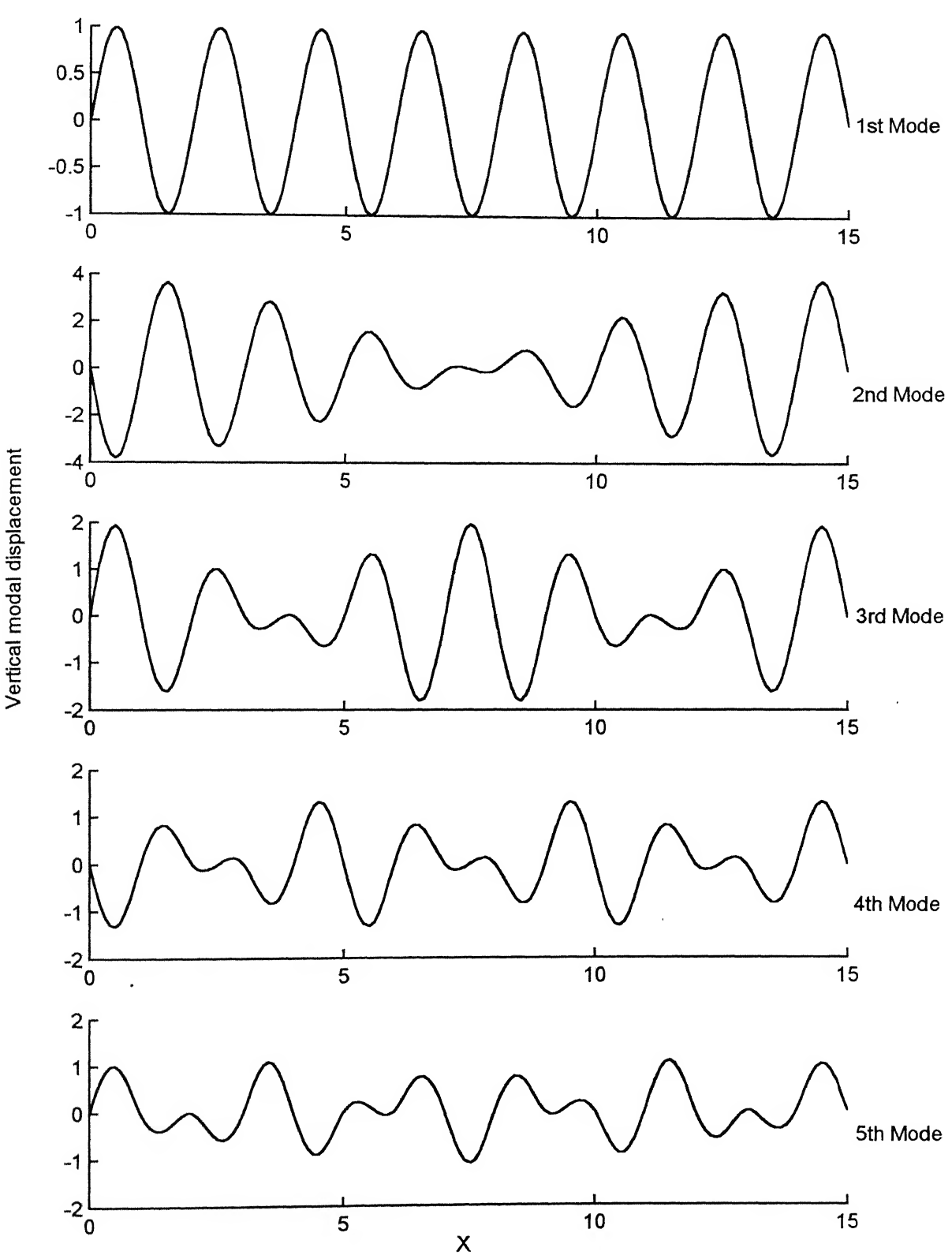

Fig 2.4 (a) Mode Shapes for 15 span beam - Analytical formulation

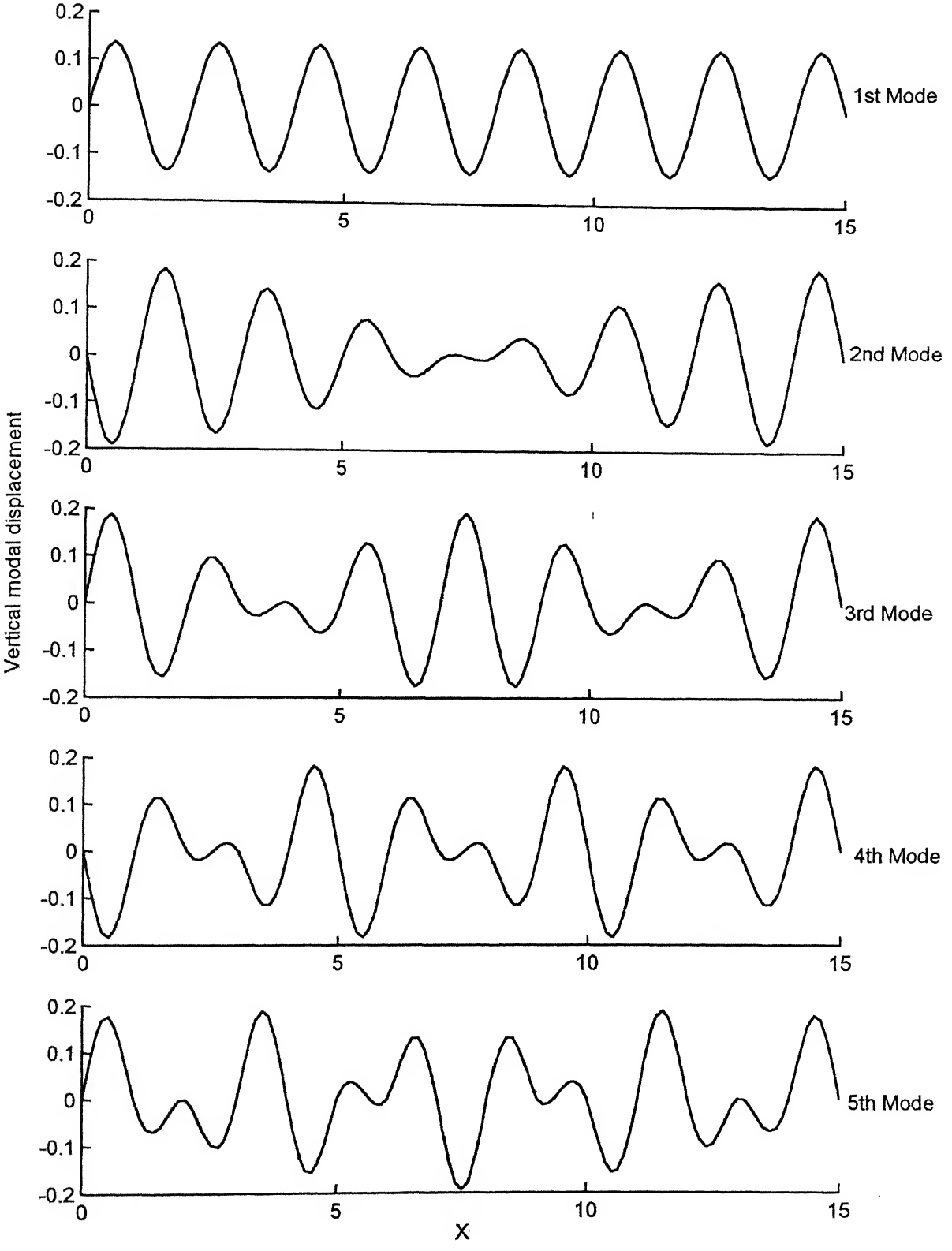

Fig 2.4 (b) Mode Shapes for 15 span beam - FE-Method

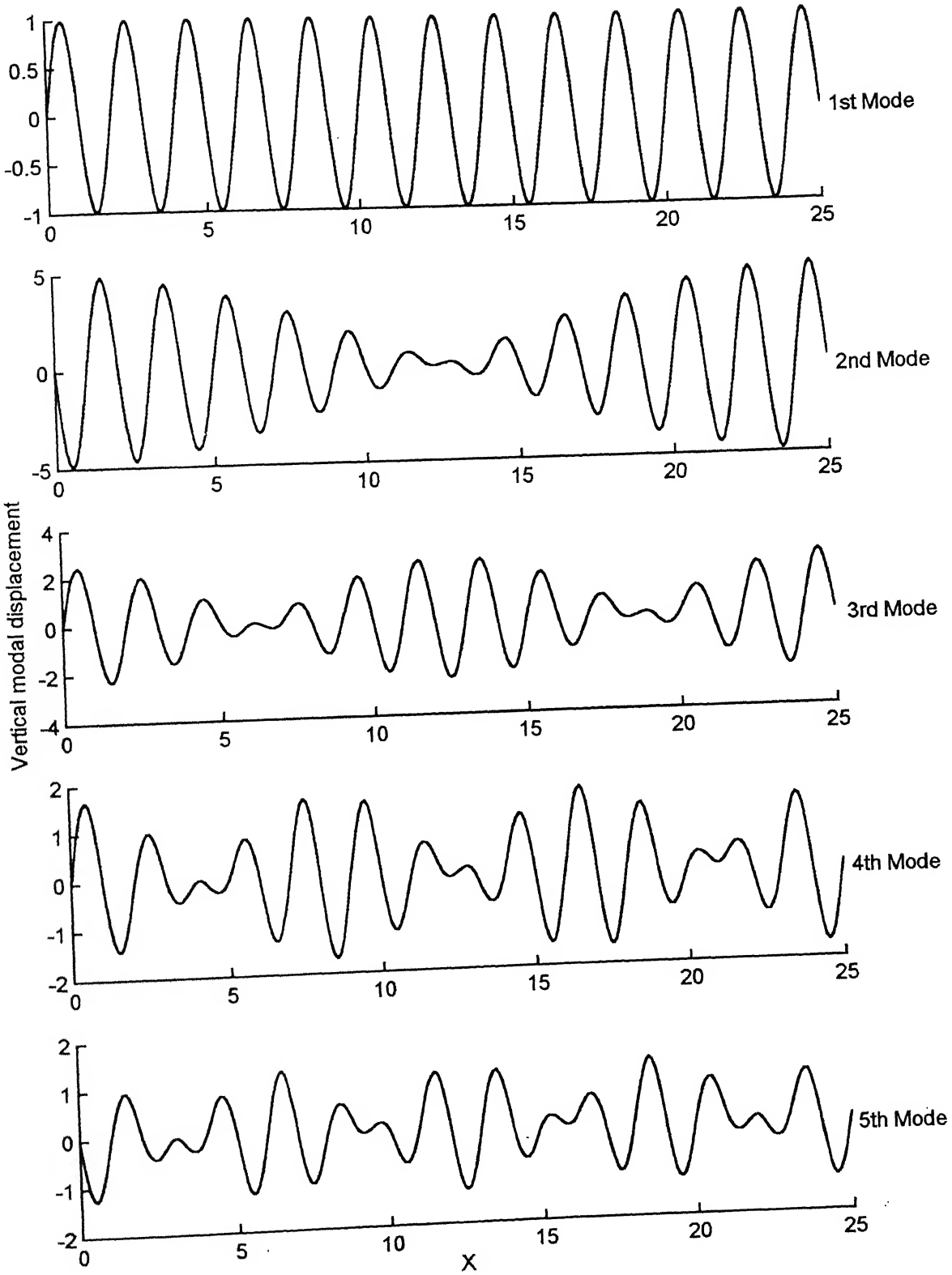

Fig 2.5 (a) Mode Shapes for 25 span beam - Analytical formulation

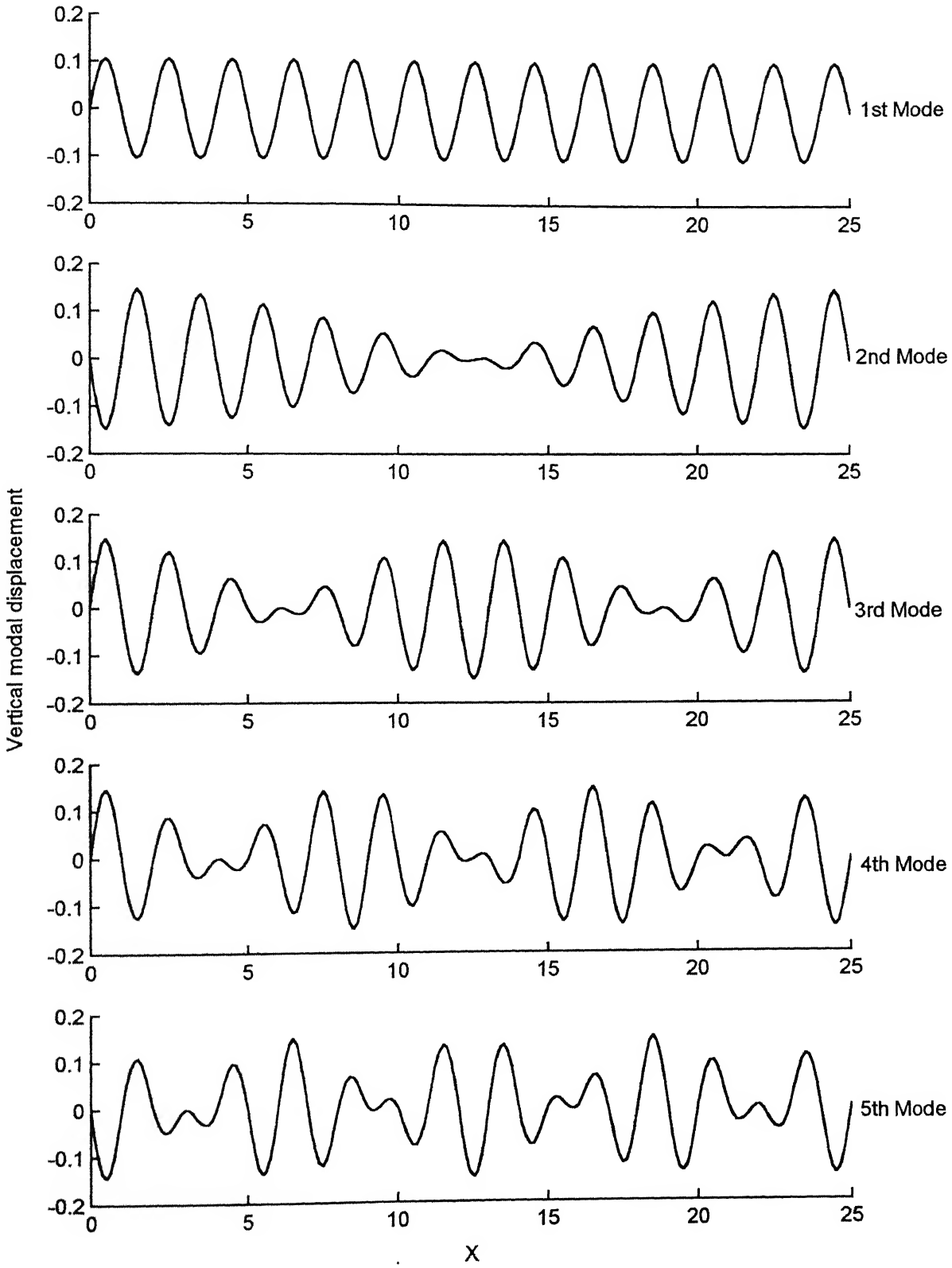

Fig 2.5 (b) Mode Shapes for 25 spans beam - FE-Method

CHAPTER 3

VIBRATION OF MULTI-SPAN CONTINUOUS BEAMS UNDER TRAVELLING LOAD

The response of multi-span continuous beams subjected to moving loads is discussed in this Chapter. Using principle of virtual work general expressions for forced vibration response (Timoshenko, 1955) are presented. These are consequently employed to express beam vibrations caused due to constant magnitude moving loads. The analytically obtained response is compared with that from the FE model.

3.1 Governing Equation

Representing the lateral vibration of a beam (Fig 3.1) subjected to external disturbing forces, by a series

$$w = \mu_1 X_1 + \mu_2 X_2 + \mu_3 X_3 + \ldots\ldots\ldots\ldots \tag{3.1}$$

in which X_1, X_2...are normal functions of the beam correspondent to the end condition of the entire vibrating beam and $\mu_1, \mu_2, \ldots\ldots\ldots$ are time functions.

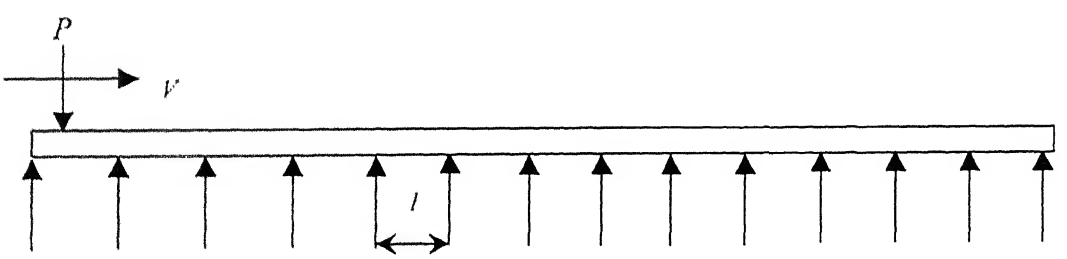

Fig 3.1 Multi spans continuos beam under a moving force

The inertia forces per unit length of the beam can be expressed as

$$-\rho A\ddot{w} = -\rho A \sum_{m=1,2,3,\ldots} \ddot{\mu}_m X_m \tag{3.2}$$

For a virtual displacement

$$\delta w = \delta \mu_m X_m \tag{3.3}$$

the virtual work done by inertia forces is

$$-\rho A\int_0^L \ddot{w}\delta w dx=-\rho A\ddot{\mu}_m\delta\mu_m\int_0^L X^2{}_m dx \tag{3.4}$$

where L is the total length of beam.

The strain energy of bending beam at any instance is

$$V_e=\frac{EI}{2}\int_0^L(\frac{d^2w}{dx^2})dx$$

which can be expressed as

$$V_e=\frac{EI}{2}\sum_m \mu_m{}^2\int_0^L X''_m{}^2 dx$$

Similarly, the virtual work done by elasticity forces can be expressed as

$$-\frac{\partial V_e}{\partial\mu_m}\delta\mu_m=-\frac{EI}{2}\mu_m\delta\mu_m\int_0^L X''_m{}^2 dx \tag{3.5}$$

For the disturbing force P applied at the distance c from the left end of beam of first span, the virtual work is

$$P(\delta w)_{x=c}=P\delta\mu_m(X_m)_{x=c} \tag{3.6}$$

Applying principle of virtual work to expressions (3.4), (3.5), (3.6), the equation of motion is obtained as,

$$\ddot{\mu}_m+\frac{EI}{\rho A}\frac{\int_0^L X''_m{}^2 dx}{\int_0^L X_m{}^2 dx}\mu_m=\frac{P}{\rho A\int_0^L X_m{}^2 dx}(X_m)_{x=c} \tag{3.7}$$

Employing the notation

$$\lambda_m{}^2 = \frac{EI}{\rho A}\frac{\int_0^L X_m''{}^2 dx}{\int_0^L X_m{}^2 dx} \tag{3.8}$$

equation (3.7) can be written as

$$\ddot{\mu}_m + \lambda_m{}^2 \mu_m = \frac{P}{\rho A \int_0^L X_m{}^2 dx}(X_m)_{x=c} \tag{3.9}$$

The general solution of equation (3.9) is

$$\mu_m = C_m \cos\lambda_m t + D_m \sin\lambda_m t + \frac{P}{\rho A \lambda_m \int_0^L X_m{}^2 dx}\int_0^t (X_m)_{x=c} \sin\lambda_m (t-t_1)dt_1 \tag{3.10}$$

where C_m and D_m are constants, which can be found from initial conditions. The third term represents the vibration produced by disturbing force.

For zero initial conditions, we get

$$\mu_m = \frac{1}{\rho A \lambda_m \int_0^L X_m{}^2 dx}\int_0^t P(X_m)_{x=c} \sin\lambda_m (t-t_1)dt_1 \tag{3.11}$$

3.2 Response to Moving Force

Consider the disturbing force P to be moving along the beam at velocity V. Let the force be at the left support of the first span of the beam, at the initial moment ($t = 0$). Then at any other time instant moment $t = t_1$, the distance of the force from the left support of the first span will be

$c = Vt_1$

The virtual work done by the moving force

$$P\delta\mu_m (X_m)_{x=Vt_1} \tag{3.12}$$

Through comparison of equations (3.12) and (3.6) and substituting $(X_m)_{x=Vt_1}$ for $(X_m)_{x=c}$ in equation (3.11), the beam response due to the moving force can be written as

$$\mu_m = \frac{P}{\rho A \lambda_m \int_0^L X_m{}^2 dx} \int_0^t (X_m)_{x=Vt_1} \sin \lambda_m (t - t_1) dt_1 \qquad (3.13)$$

3.3 Numerical Examples

The response is numerically computed through the procedure outlined and compared with the Finite Element Model developed in NISA. This comparison is carried out to validate the finite element model. For the multi-span beam, earlier specified in section 2.4, the forced vibration response is numerically computed for the following set of data:

Case 1:

Total number of spans N	15
Moving load P	10 N
Total number of modes considered	12
Velocity, V of the moving load	2.5 m/s

The response at the mid point of the central span (r = 8) obtained through the analytical procedure and the finite element method (NISA) are plotted in Figs 3.2 (a) and (b), respectively.

Case 2:

Total number of spans N	15
Moving load P	10 N
Total number of modes considered	12
Velocity, V of the moving load	5.0 m/s

The response at the mid point of the central span (r = 8) obtained through the analytical procedure and the finite element method (NISA) are plotted in Figs 3.3 (a) and (b), respectively.

The response obtained from the analytical formulation and the FE models can be seen to be identical for both cases. This is taken as a pointer to the correctness of the finite element modeling procedures developed using NISA.

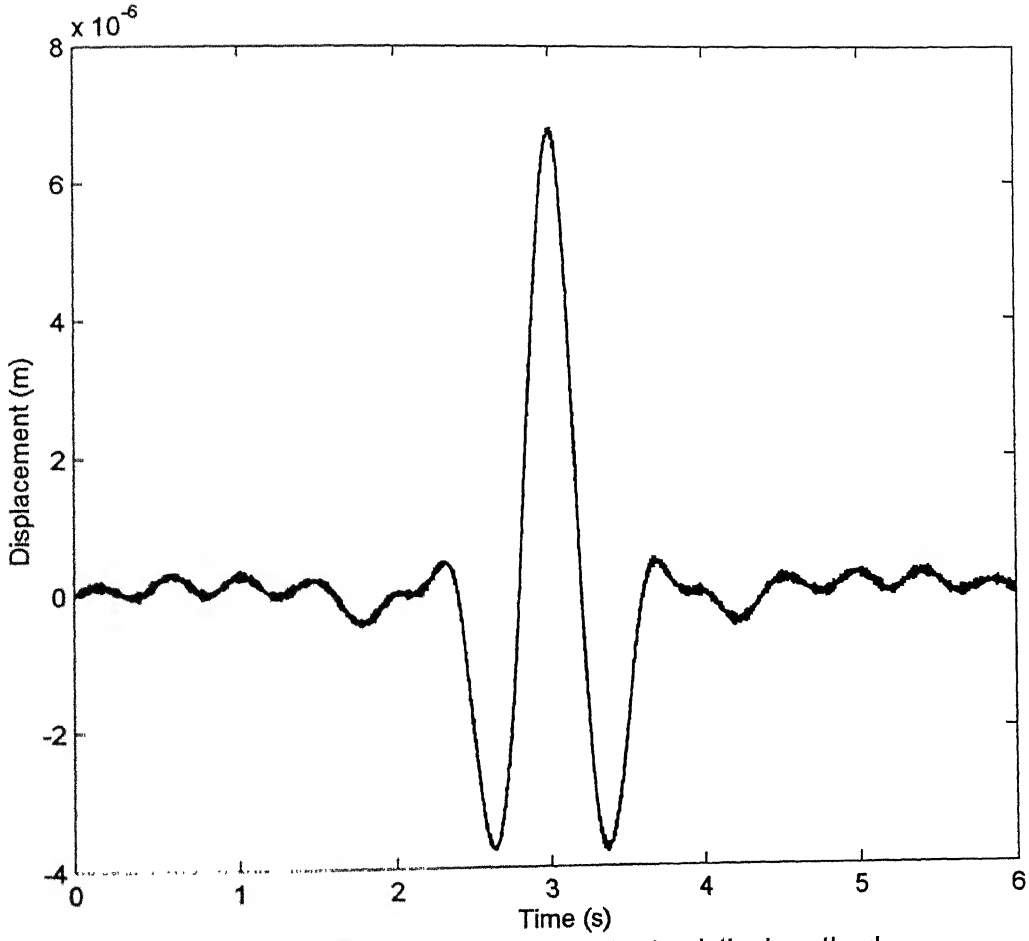

Fig 3.2 (a) Response for Case 1 - Analytical method

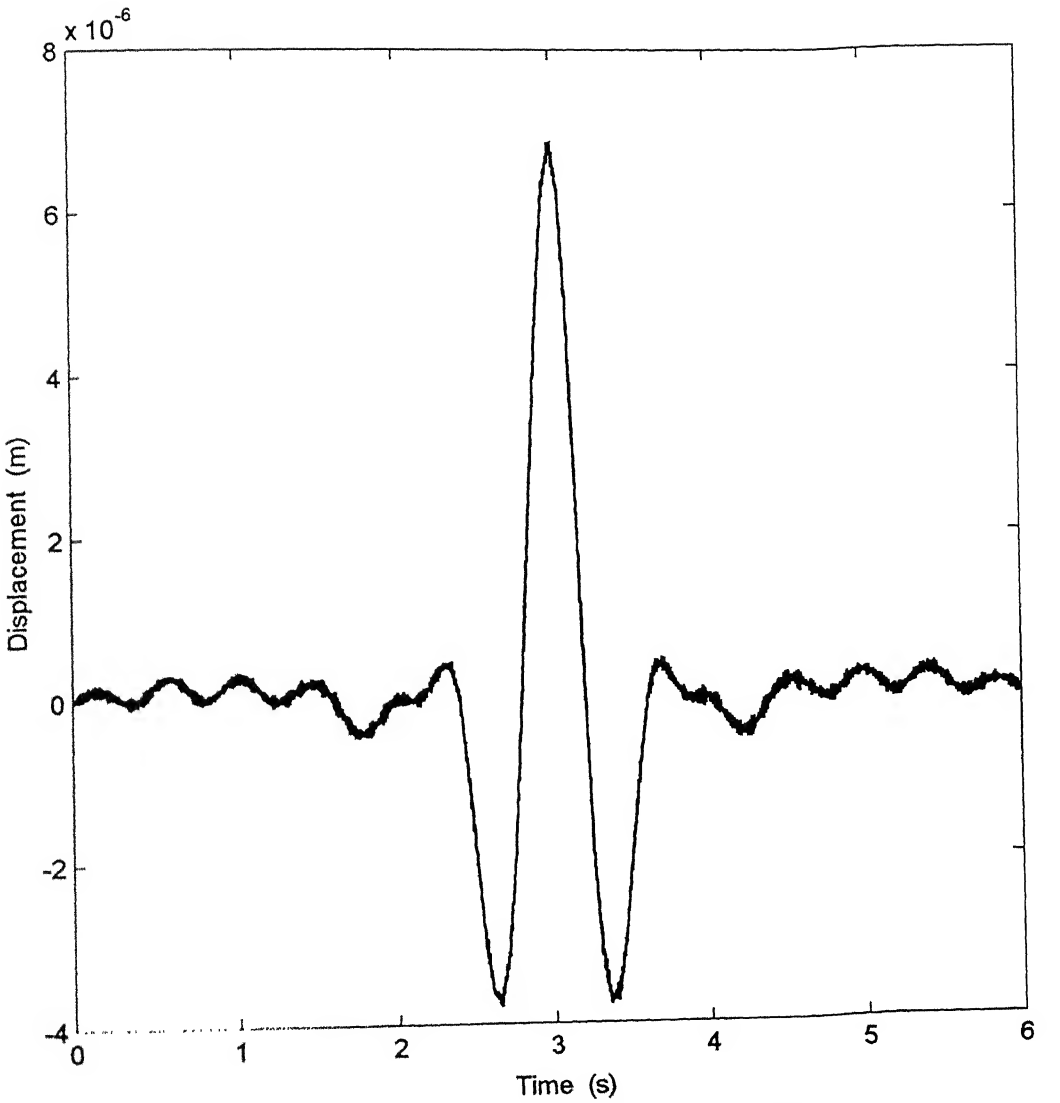

Fig 3.2 (b) Respose for Case 1 - FE-method

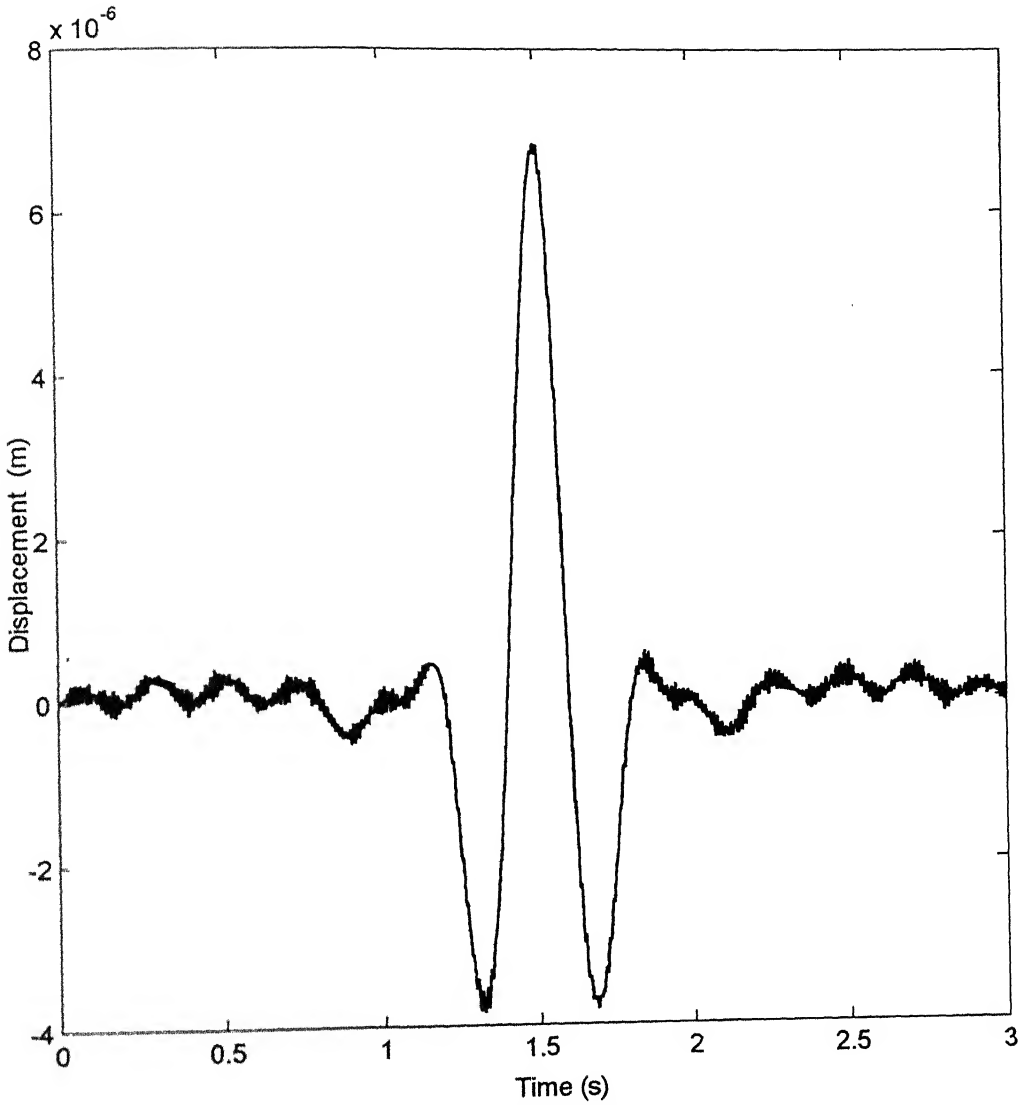

Fig 3.3 (a) Response for Case 2 - Analytical method

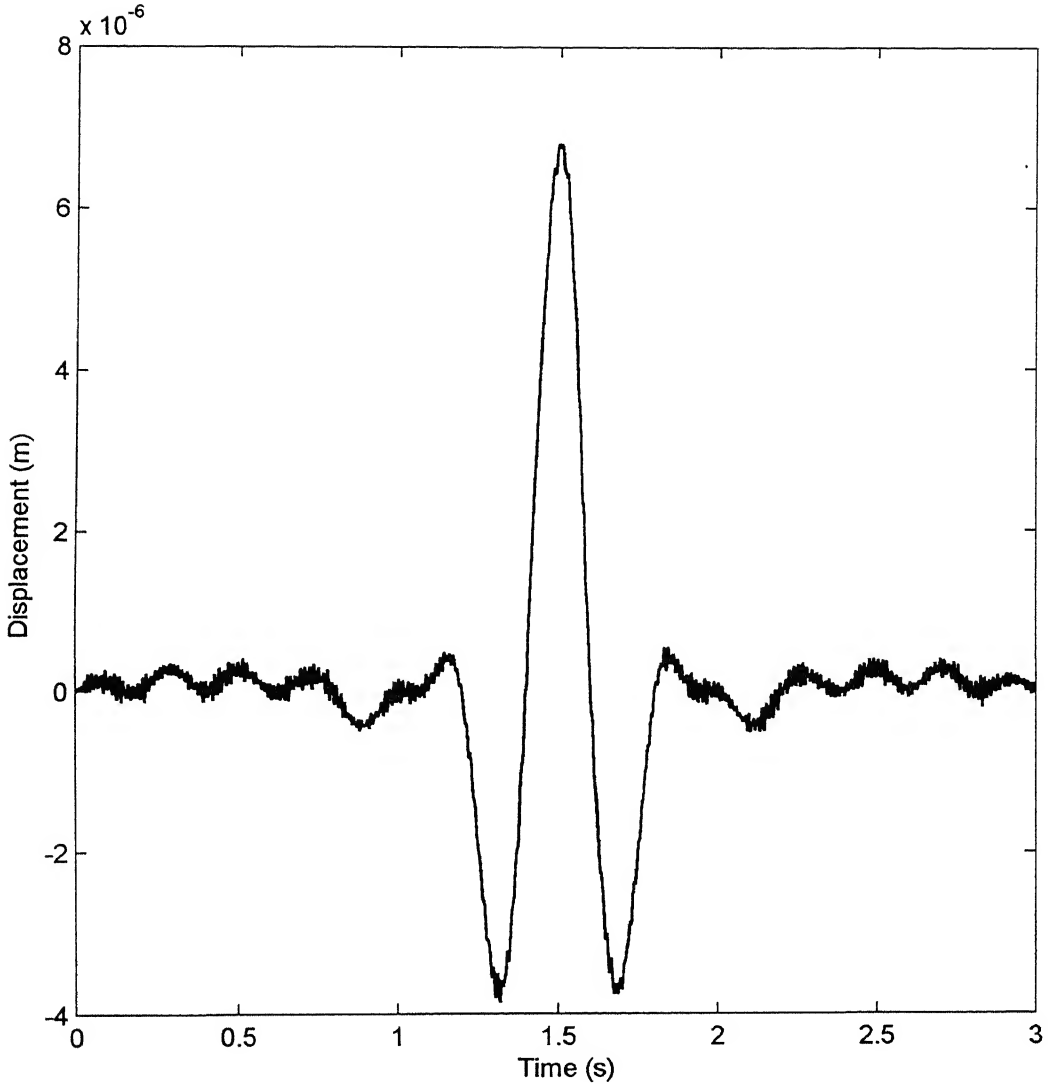

Fig 3.3 (b) Response for Case 2 - FE-method

CHAPTER 4

RAIL RESPONSE UNDER WHEEL-FLAT LOADING

Rail response under wheel-flat excitation has been investigated. Initially the rail vibration under loading due to normal wheels is investigated. The analysis is consequently extended to incorporate loading due to wheels, which have developed flats. Modeling is done through the Finite Element package NISA and the wheel loads are treated as moving loads.

4.1 Railway Data

Analysis is carried out for typical data obtained from Indian Railways. A railway train comprising of an engine and one wagon are considered. A schematic of the train is given in Fig.4.1 (a). The engine has 12 wheels (six wheels on either side). On each side there are three front wheels and three rear wheels. Each wagon has eight wheels, four on either side, each side having two front wheels and two rear wheels. Analysis is carried out for only one side of the railway track (the response on the other side being identical). The rail cross-section is shown in Fig. 4.1 (b). The data employed for the analysis is listed below:

Cross section Area of rail	66.15×10^{-4} m^2
Moment of inertia about N.A:	2158×10^{-8} m^4
Distance between two-sleeper pad	0.6 m
Young modulus of rail	2.0678×10^{11} N/m^2
Density of rail	7600 Kg/m^3
Speed of train	36 km/h (=10m/s)
Wheel diameter	1 m
Total load on each wheel of engine	92214 N
Total load on each wheel of wagon (empty)	29062.125 N
Total Number of wheels in the engine	12
Total Number of wheels in the wagon	8
Equivalent damping ratio of rail (rigid support)	0.05
Stifness of sleeper pad	2.5×10^{8} N/m
Equivalent damping ratio of rail(flexible support)	0.1

The weight of the engine and wagon is taken to act on the rail through the wheels as point forces. The respective weights of the engine and wagon are assumed to be equally distributed among the wheels. At the initial time instant the first wheel of the engine is assumed to be at node 1 of span number 1 of the rail. Table 4.1 gives the wheel loading data for all the ten wheels (6 from engine and 4 from the wagon).

Table 4.1 Wheel loads, distances and arrival times at node 1
(Train velocity =10 m/s)

Wheel No.	Arrival time at node 1 (s)	Wheel load (*k*N)	Distance from first engine wheel (m)
1	0.00	92.214	0.0
2	0.21	92.214	2.1
3	0.42	92.214	4.2
4	1.05	92.214	10.5
5	1.26	92.214	12.6
6	1.47	92.214	14.7
7	1.79	29.062	17.9
8	1.99	29.062	19.9
9	2.44	29.062	24.4
10	2.64	29.062	26.4

Total time taken to cross rail by train = (rail length + train length) /velocity

= (9 + 26.4)/10 = 3.54 s

4.2 Finite element modeling

Two models of rails are developed, namely (i) rail with rigid supports (ii) rail with flexible supports. A rail track of 15 spans is considered. The length of each span is 0.6 m. Different scenarios with wheel flat falling on the supports and in-between supports, are discussed. Details of the FE model are given below:

(i) Rail with rigid support

Type of element	2-D beam
Order of element:	1 (linear)
Number of degrees of freedom per node of beam element	3 (u_x, u_y, r_z)
Number of nodes per element:	2
Total number of elements in rail	118

Total number of nodes in rail	119
Total length of rail	9 m

u_x=0 is taken at all nodes of rail and u_y=0 at supports only

(ii) Rail with flexible supports

(in addition to the data of case (i))

Type of element of spring	2-D translation
Order of spring element	1(linear)
Number of degree of freedom per node of spring element:	2 (u_x, u_y)
Number of nodes per spring element	2
Total number of spring elements	15

u_x=0 is taken at all nodes of rail and u_y=0 at one end of spring element only

Finite element modeling of rail with rigid supports and flexible supports are shown in Fig 4.2 (a) and Fig 4.2 (b) respectively.

4.3 Free vibration characteristics of rail

Eigenvalue analysis of the rail was carried out in NISA using conventional subspace iteration and consistent mass formulation. Table 4.2 gives the first five natural frequencies of rail for the rigid support and flexible support models. The corresponding mode shapes are given in Figs. 4.3 (a) and (b).

Table 4.2 First five natural frequencies of rail (rad/s)

Mode No.	Rigid support	Flexible support
1	7842.73	2854.00
2	7941.44	2854.11
3	8230.34	2862.73
4	8690.14	2891.54
5	9295.03	2955.22

4.4 Wheel flat loading

The loading pattern caused due to out-of-roundness of the wheel depends on the severity and shape of the damage on the wheel. The out-of-roundness is however idealised by a flat on the surface, which would be seen as a chord on circular profile of the wheel. Such

a flat results in loss of contact between the wheel and the rail for a short time and then regaining of contact. This idealised lift and hit phenomenon is shown in Fig. 4.4. When there is no contact, the wheel rises above the rail until contact is recovered resulting large impact force. However, due to the bogie suspension system, the loss of contact between the wheel and the rail is not total as the wheel moves downwards and the rail upwards to compensate for the absence of wheel material. The overall effect is that the contact surface initially decreases and later due to inertia, the wheel continues downward motion resulting in an increase of contact force. The maximum and minimum values of normalized contact force between the wheel and the rail, for various speeds were calculated by Neilsen and Igeland (1995) and are reproduced here in Fig. 4.5.

4.5 Vibration of rail under moving train

Rail vibration under the moving train has been computed in terms of deflection and acceleration. The ten point loads from the ten wheels are moving on rail simultaneously. Response has been computed for the following cases:

1 Undamped System
   (a) without flat
   (b) with flat
2 Damped System
   (a) without flat
   (b) with flat

The wheel flat is assumed to be present on the 10^{th} wheel of the train. The chord length of the flat is taken as 60 mm. The forced vibration analysis is carried out in NISA and 30 modes are taken under consideration. Modes beyond 30 are found to have negligible influence on the response for the train velocity of 10m/s (=36 Km/hr), under consideration.

The wheel-flat hits on the rail on the 5^{th} and then on the 10^{th} spans. In order to improve accuracy of results 20 element are taken on these spans, while on the remaining spans the number of finite beam elements are 6. Thus, the response is computed for 119 nodes on

the rail. The loading patterns for the case with and without wheel flats are shown in Figs.4.6 (a) and (b) for 5^{th} and 10^{th} span respectively. The flat wheel looses at node 33 and regains it at node 35. Again, it looses contact at node 82 to regain it at node 84.. The nodal distances and arrival time of the 10^{th} wheel at these nodes along with the tenth node (which sees normal wheel behaviour) are listed in Table 4.3.

Table 4.3 Nodal distances and arrival time of 10^{th} wheel

Node Number	Distance from Node 1 (m)	Arrival time of the 10^{th} wheel (s)
10	0.90	2.730
33	2.64	2.904
34	2.67	2.907
35	2.70	2.910
82	5.79	3.219
83	5.82	3.222
84	5.85	3.225

Node 35, where the hit occurs for the first time, lies in the centre of a beam span (number 5). Node 84, where the hit takes place for the second time is close to a support (i.e. a sleeper). The vibration of rail is expected to be more due to the first hit, in comparison to that due to the second hit.

For the undamped system with rigid supports the displacement response at nodes 10, 33 and 35 is shown in Figs. 4.7 (a), (b) and. (c) corresponds to the normal case (without flat) and Figs 4.8 (a), (b) and (c) gives the response in the case of a wheel with flat.

The corresponding acceleration response is shown in Figs. 4.9 (a), (b) and (c) and 4.10 (a), (b) and (c). It can be seen that while each wheel causes distinct deflection as it passes through each node, the acceleration response does not provide a clear picture since it comprises of a large number of frequency components. It can be said that measurement of displacement response through strain gauging techniques can provide better information than that obtained through measuring acceleration, using accelerometer sensors.

From the plots of Figs. 4.8 (b), the impact caused by the wheel flat is clearly visible. The maximum deflection due to the engine wheels is 47.82 μm at node 35. Maximum deflection, at node 35, due to the wagon wheels is 15.59 μm in the absence of any flat, while it rises to 27.35 μm, when a flat is present. Occurrence of this increase in the maximum deflection can serve as an effective tool for wheel-flat detection. The zoomed picture of the response under wheel flat loading is depicted in Fig.4.11, which clearly indicates the lift and hit mechanism of the wheel flat discussed earlier.

The response for the damped system is shown in Figs. 4.12 (a), (b) and (c). The inclusion of damping in the analysis, as can be seen, removes the free vibration components, from the response plots. The zoomed picture of the response under wheel flat loading is given in Fig.4.13.

Computation is also carried out for cases where the rail support has been taken as flexible. The response in this case is shown in Figs. 4.14 (a), (b) and (c). As expected deflection is higher in this case in comparison to that of the rail on rigid supports.

The response at nodes 82, 83, 84 (for rigid supports and with damping) is shown in Figs. 4.15 (a), (b) and (c). Comparison with the response at nodes 33, 34, 35, discussed earlier reveals that the deflection levels are lower and the impact due to wheel flat is also less pronounced. This is due to the fact that while nodes 33,34,35 lie in the centre of a beam span, nodes 82, 83, 84 are closer to a support (i.e. sleeper).

The maximum deflections caused by the wagon wheel, in various cases discussed above are listed in Tables 4.4 for quick comparison.

Table 4.4 Maximum deflection due to wagon wheel
(at node 35) in μm

Type of support	Without flat		With flat	
	Undamped	Damped	Undamped	Damped
Rigid support	15.59	14.89	27.35	26.26
Flexible support	221.26	79.67	203.00	109.75

4.6 Remarks

The finite element algorithm has been developed to understand the experimental results obtained from a test site. The tests have been carried out through strain-gauge instrumentation of railway track. Signals have been obtained from these sensors during passage of the train under discussion. Strain-gauge response obtained at the test site is shown in Fig. 4.16 (a) - for all normal wheels, (b) - for a 60 mm flat on wheel number 10 Fig 4.16 (c) - magnified plot of the response in (b). The deliberately introduced flat on the test wheel has been shown in Fig 4.17. The test results help to show that the Finite Element algorithm has been correctly able to model the rail vibration phenomenon under wheel-flat excitation.

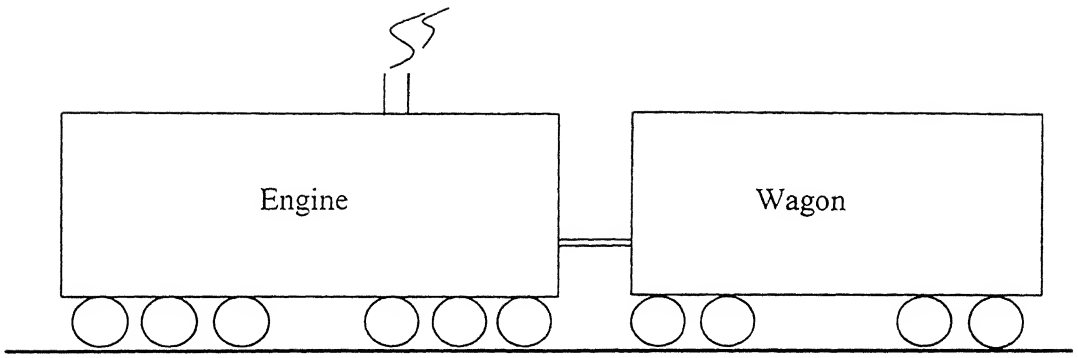

Fig 4.1 (a) Schematic Diagram of Train

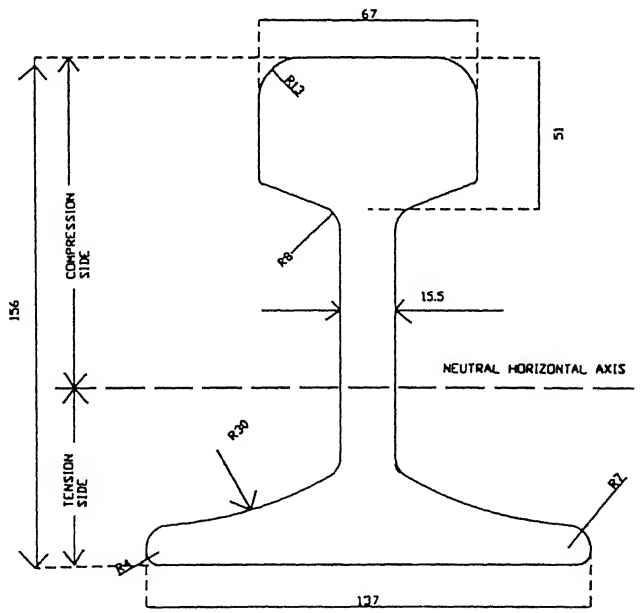

(All dimensions are in mm)

Fig 4.1 (b) Rail Section

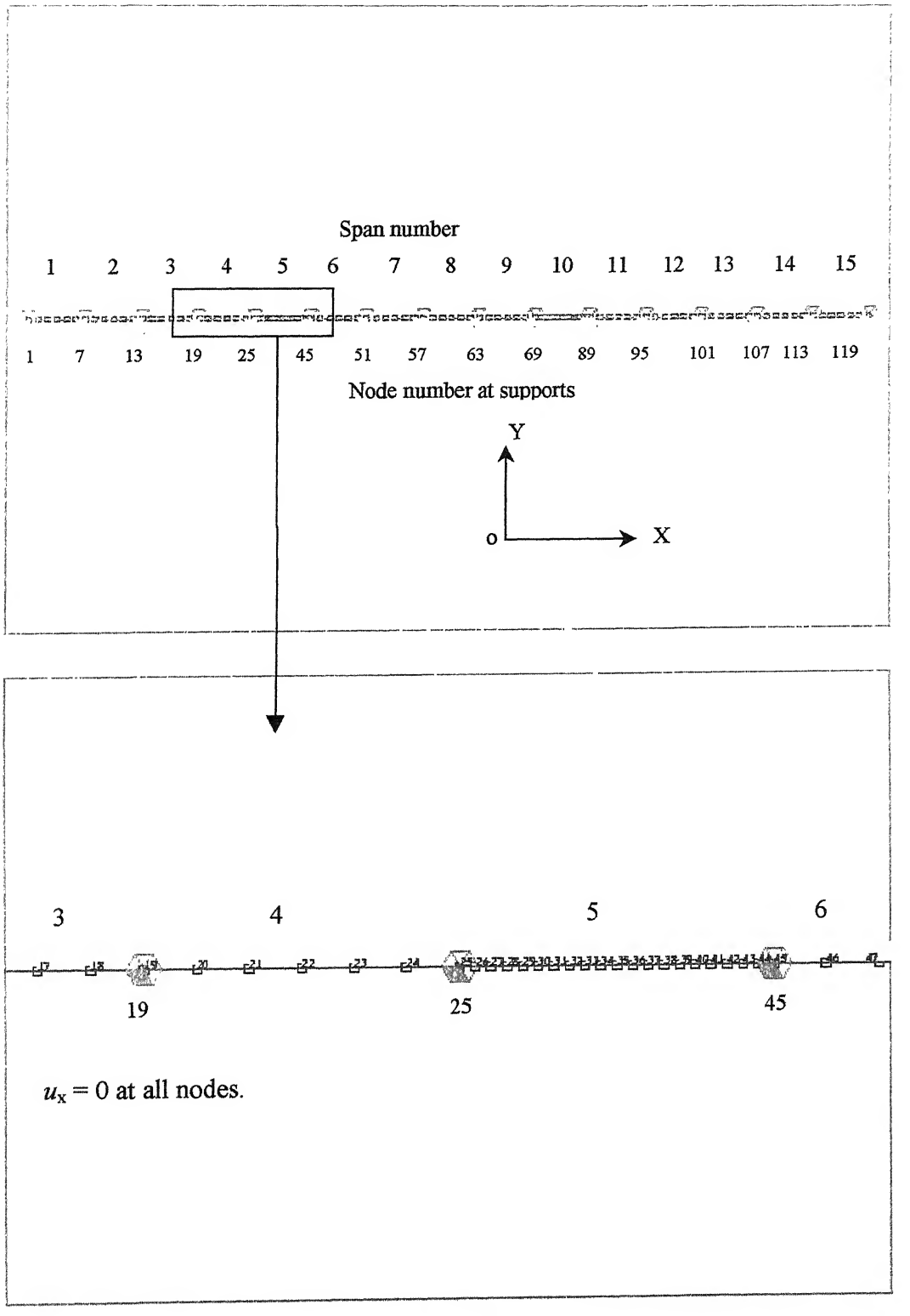

Fig 4.2 (a) Finite element Model of 15 Spans Rail - Rigid Supports

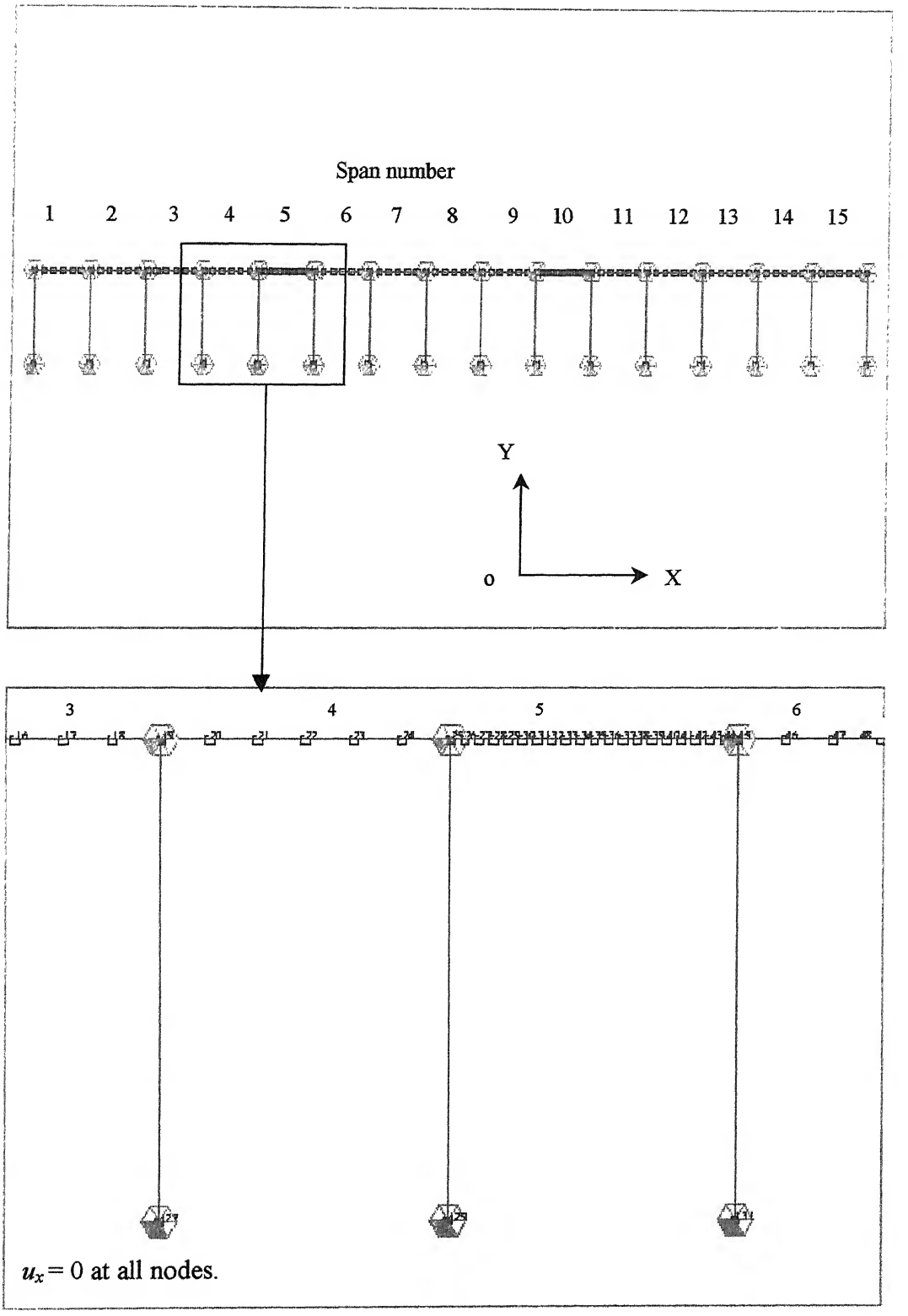

Fig 4.2 (b) Finite element Model of 15 Spans Rail - Flexible Supports

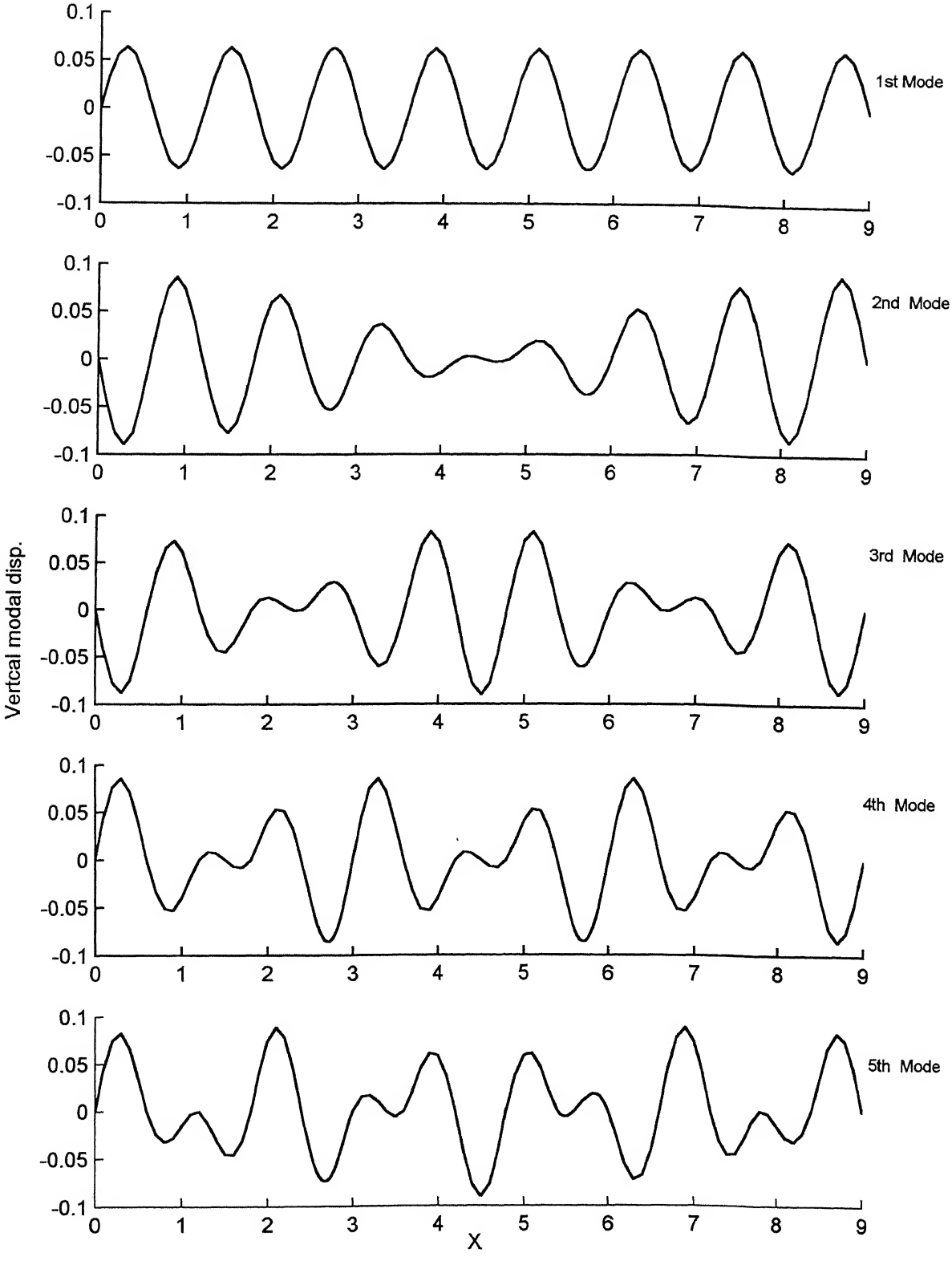

Fig 4.3 (a) Mode shapes of Rail - Rigid supports

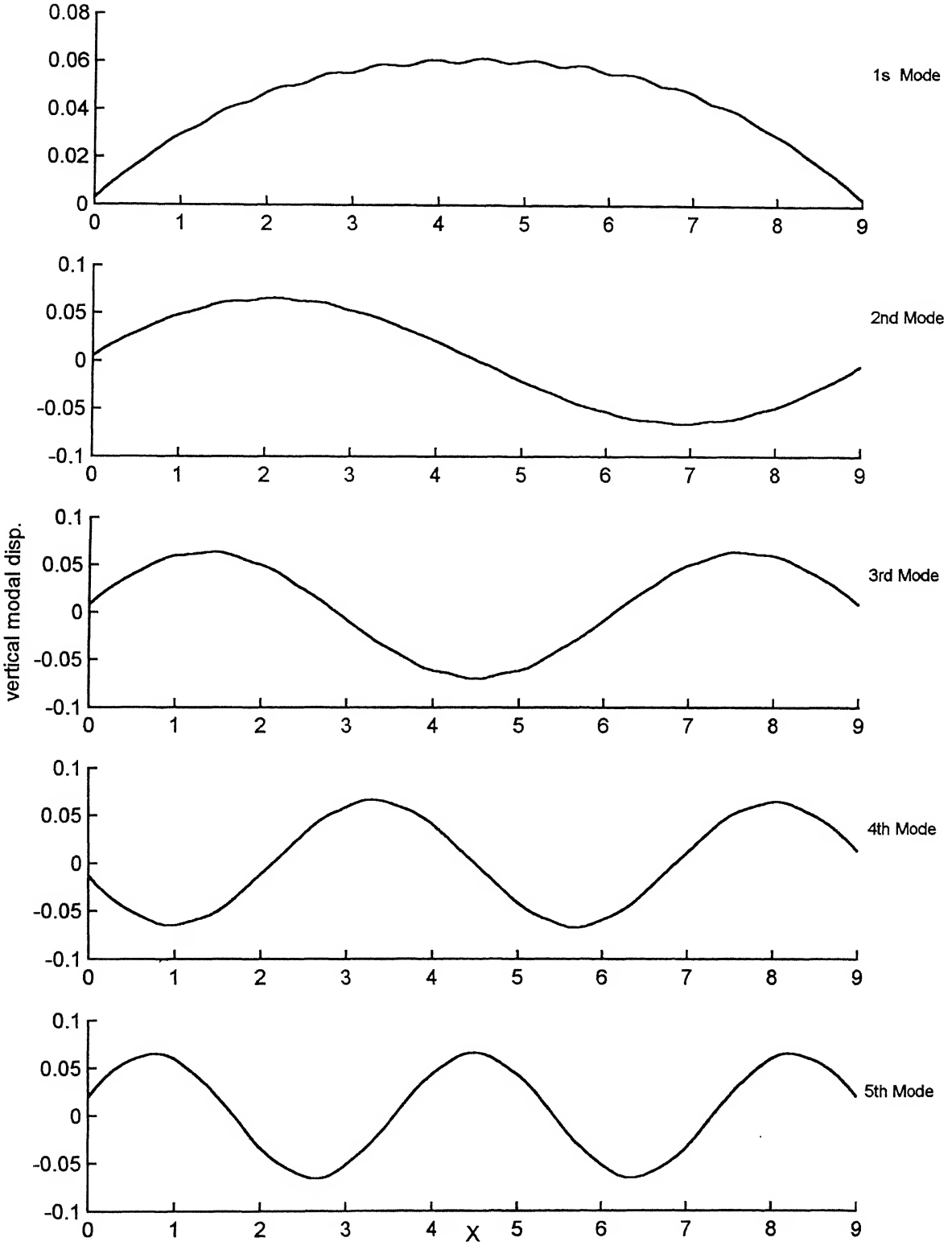

Fig 4.3 (b) Mode shapes of Rail -Flexible supports

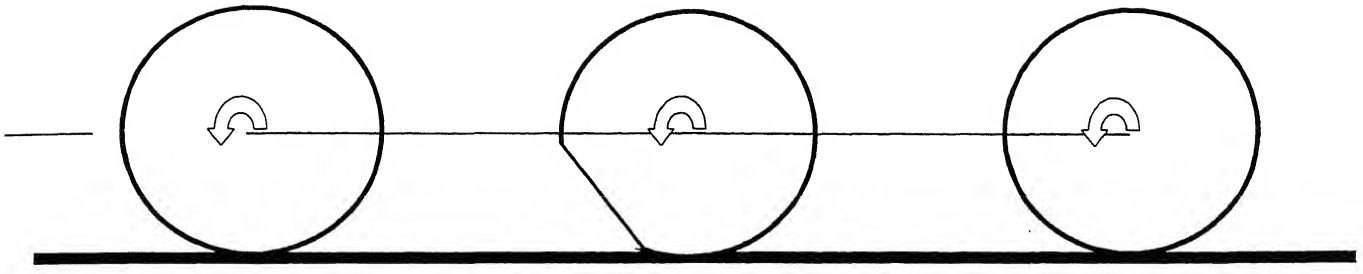

(a)

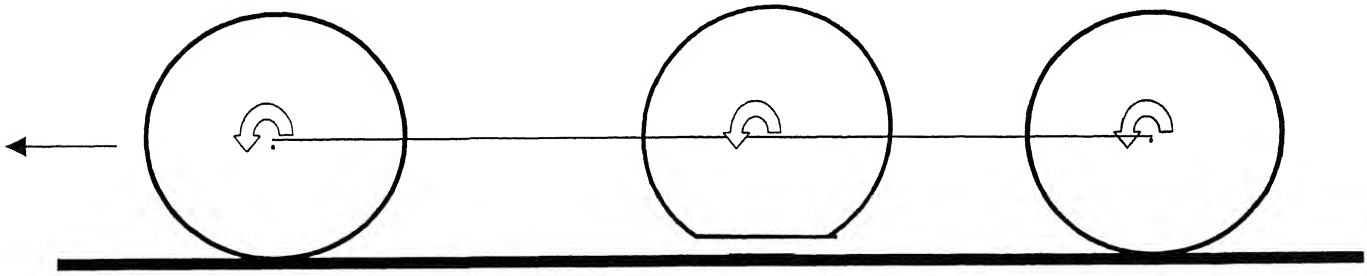

(b)

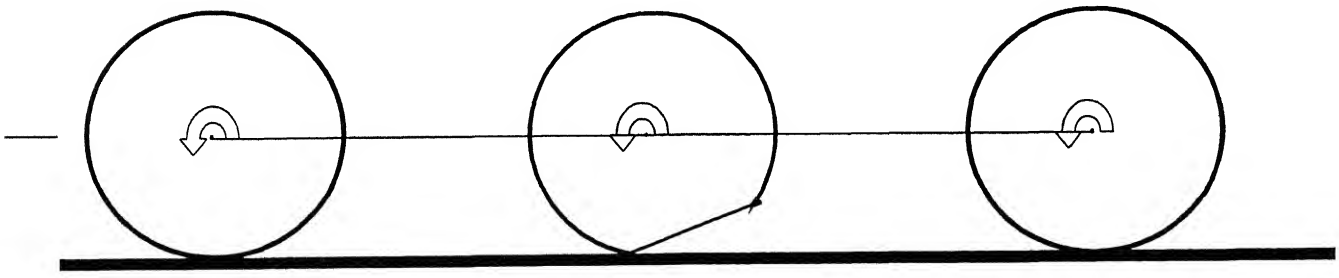

(c)

Fig 4.4 Lift and hit phenomenon of Flat wheel

(a) Start of lift, (b) lift condition and (c) hit condition

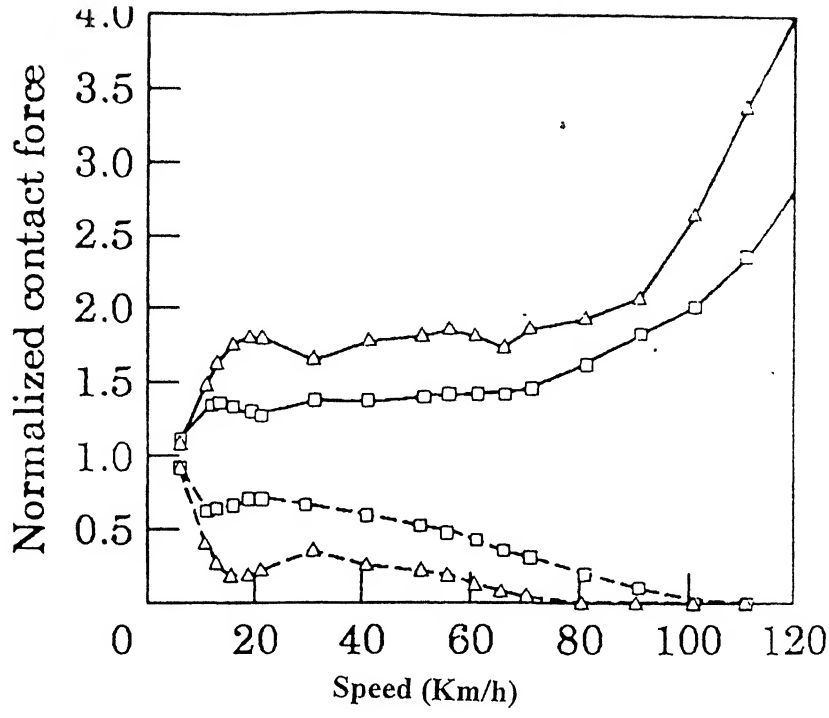

(a)

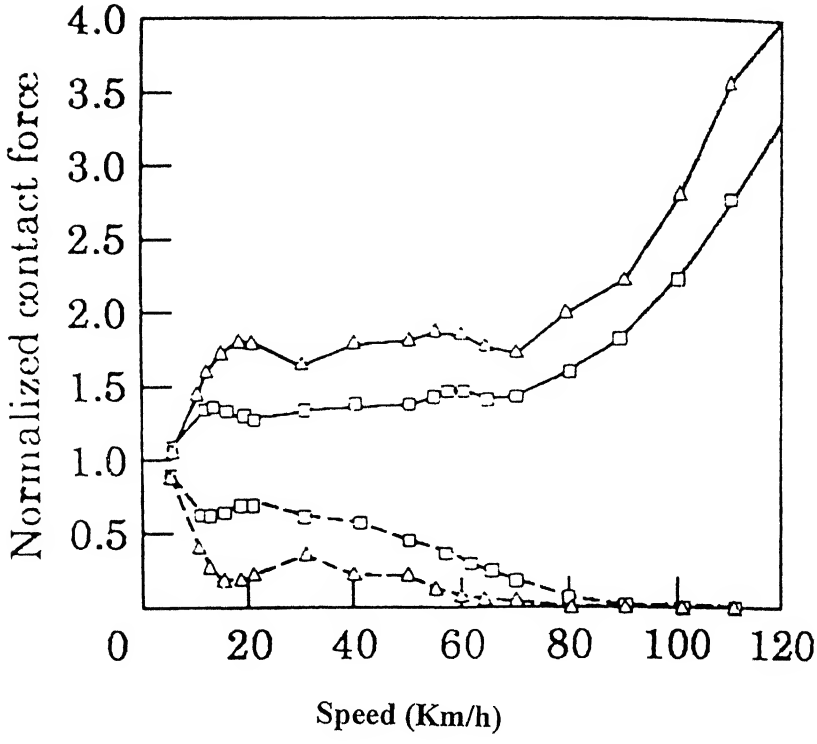

(b)

Fig 4.5 **Maximum and minimum values of contact force between wheel and rail due to wheel flat (Neilsen and Igeland, 1995)**
(Contact forces are normalized with respect to half the static axle load.
(a) one wheel flat hit midway between sleeper and (b) one wheel flat hit above sleeper. □, Wheel flat 60mm, Δ, wheelflat 90mm)

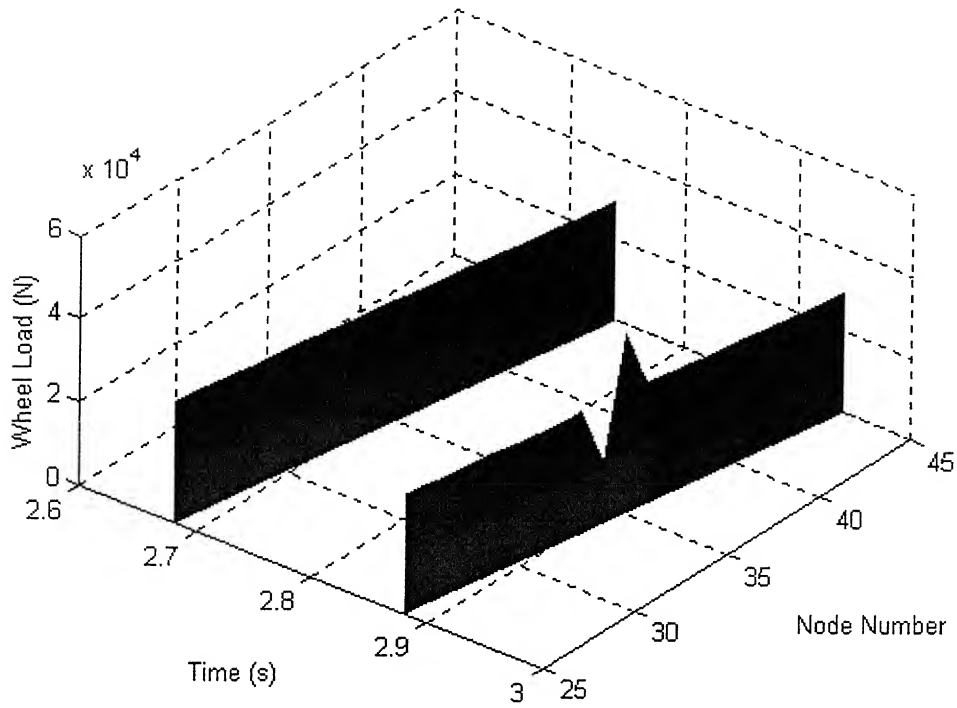

Fig 4.6 (a) Load history graph of 5th span under 9th and 10th wheel

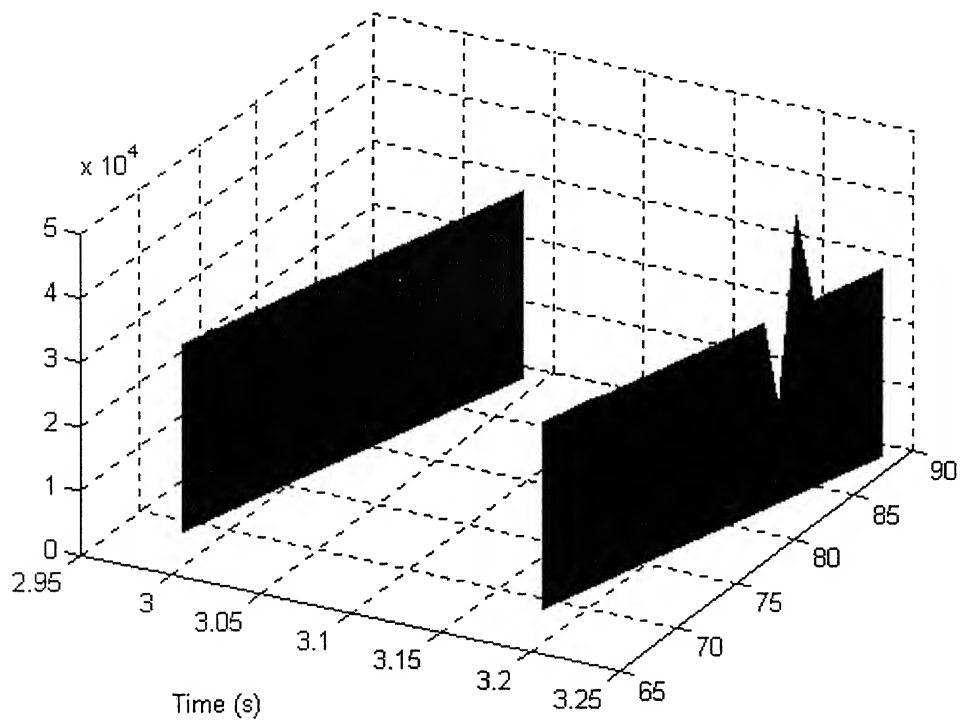

Fig 4.6 (b) Load history graph of 10th span under 9th and 10th wheel

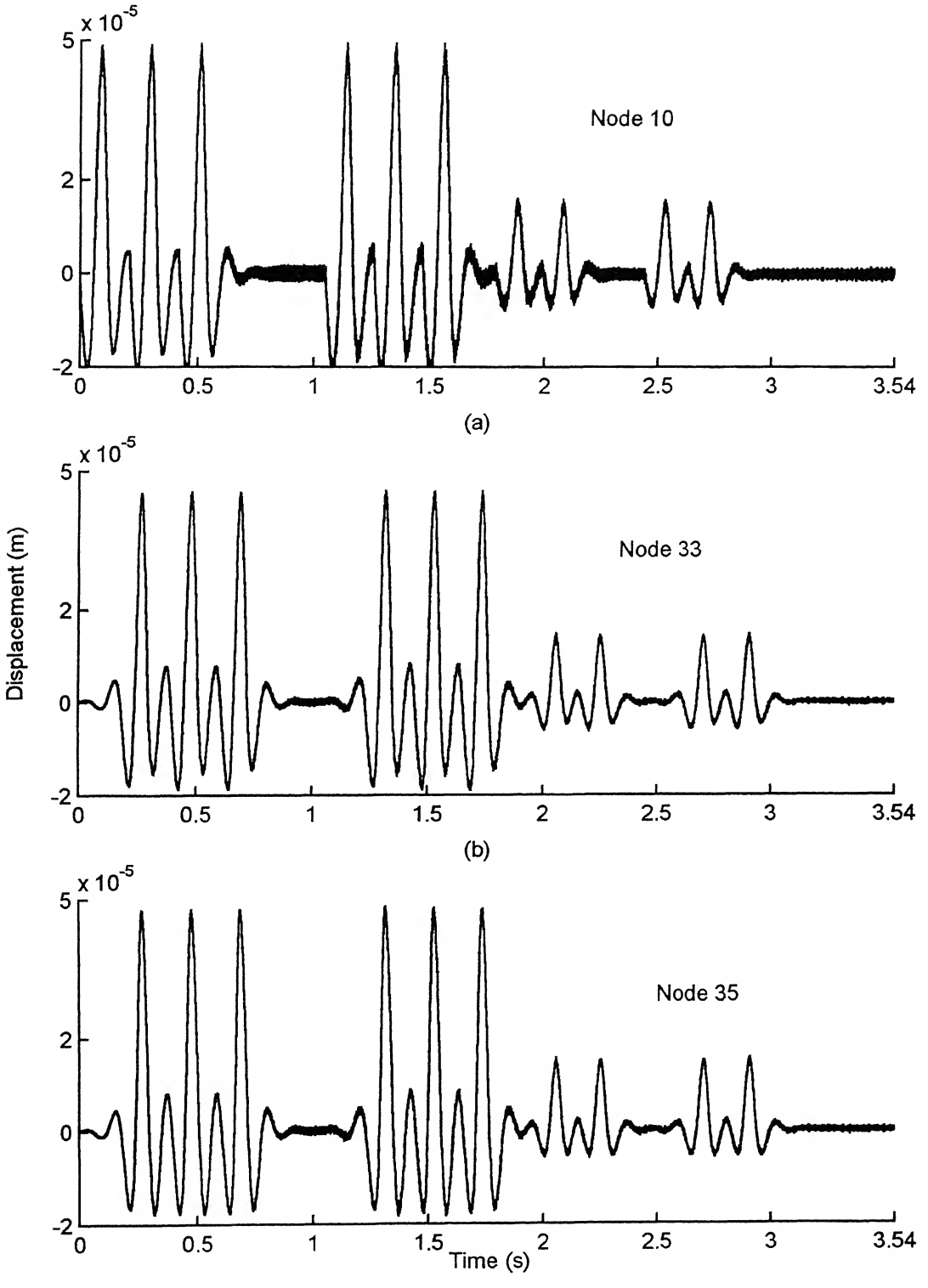

Fig 4.7 Rail Response for Case 1 (a) - Rigid supports

(a) node 10, (b) node 33 and (c) node 35

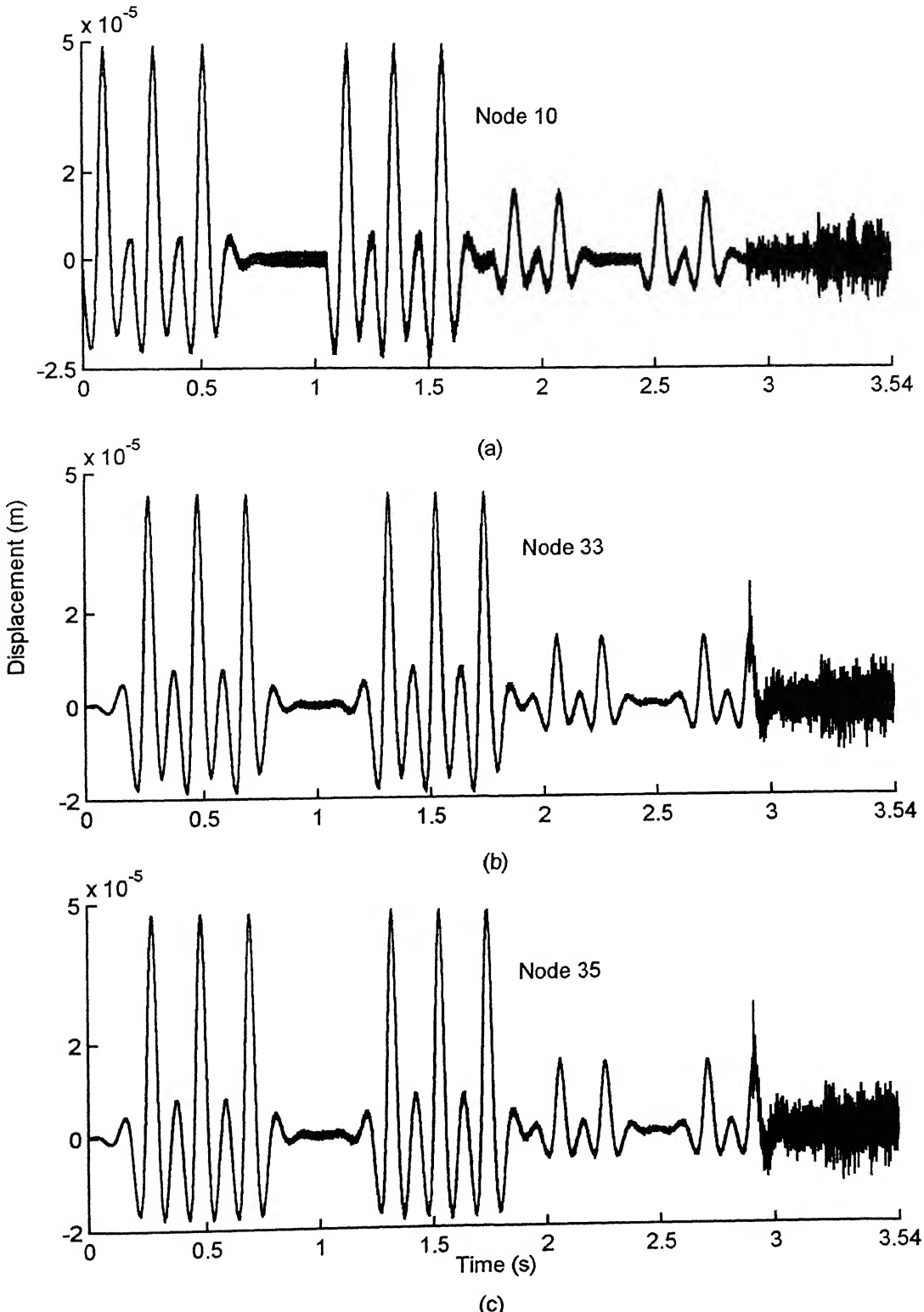

Fig 4.8 Rail Response for Case 1 (b)-Rigid supports
(a) node 10, (b) node 33 and (c) node 35

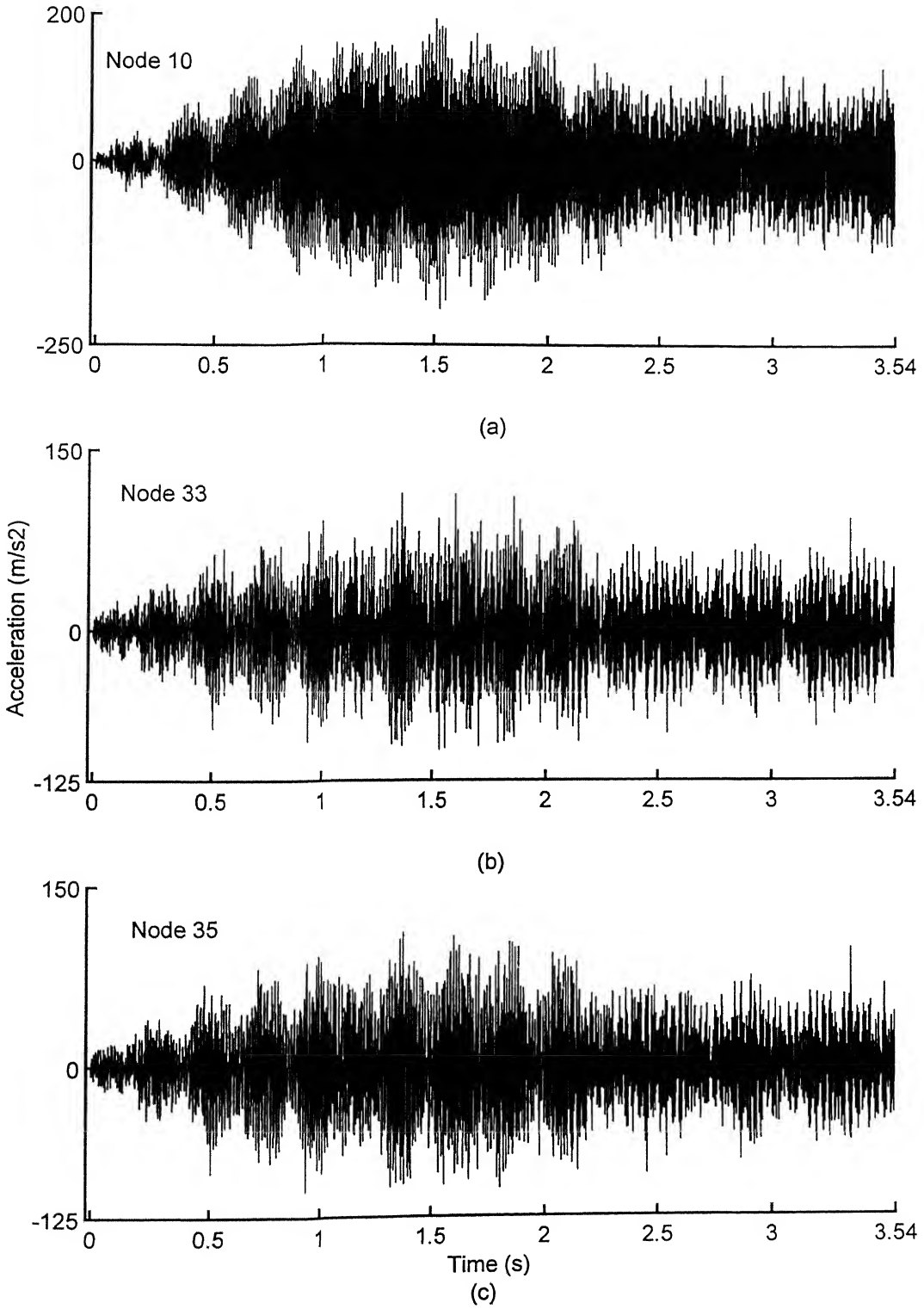

Fig 4.9 Acceleration Response for Case 1 (a) - Rigid supports
(a) node 10 , (b) node 33 and (c) node 35

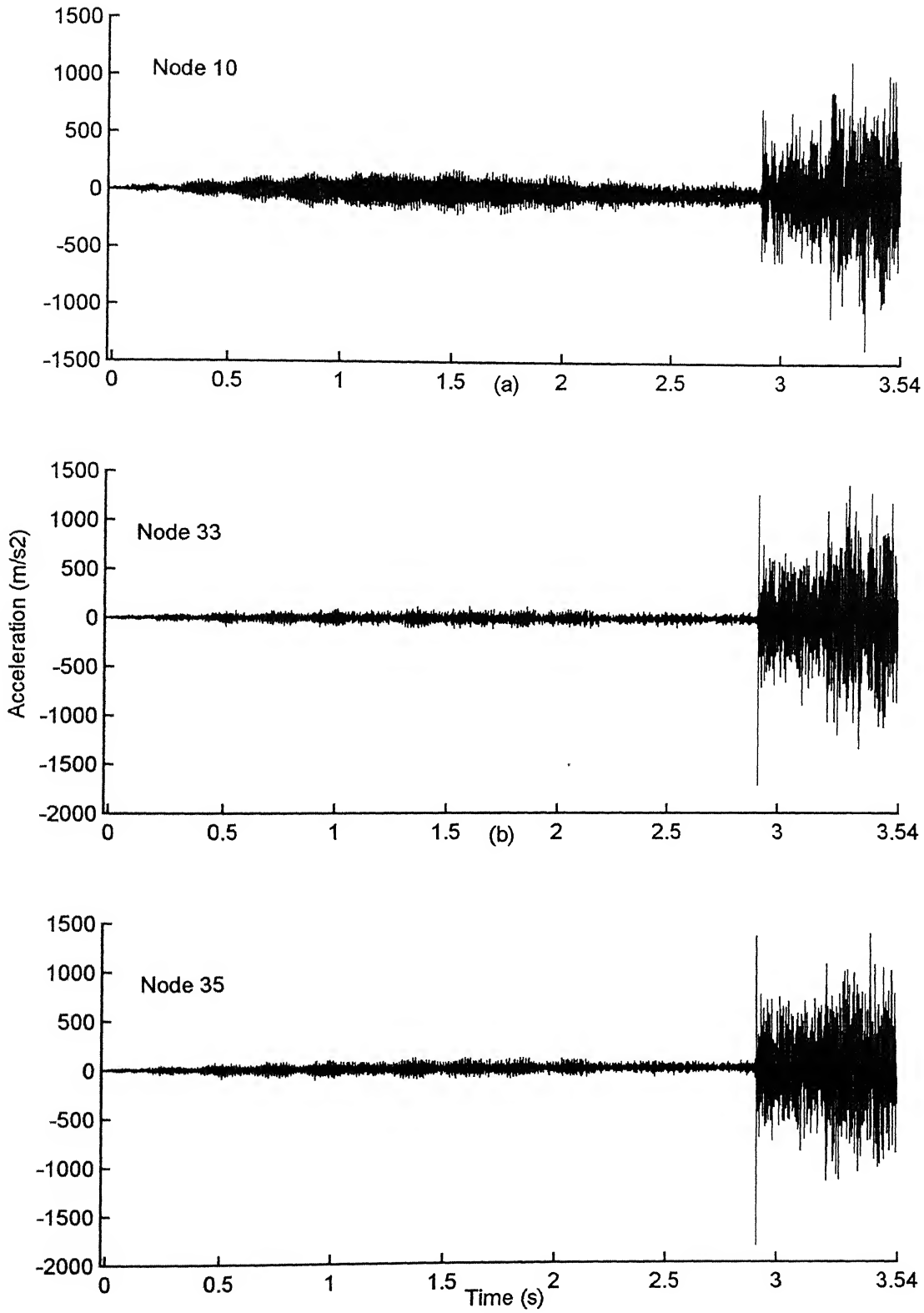

Fig 4.10 Acceleration Response for Case 1 (b) - Rigid supports
(a) node 10, (b) node 33 and (c) node 35

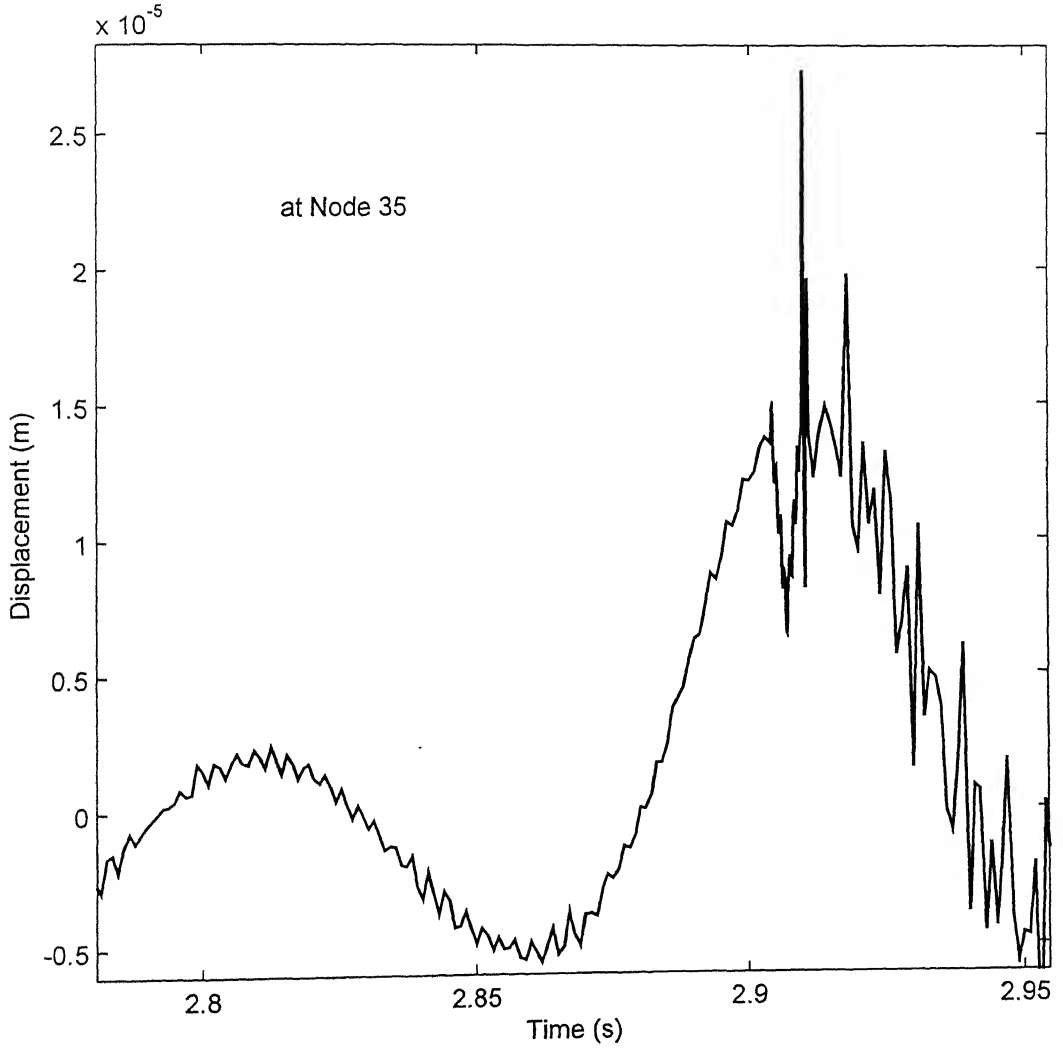

Fig 4.11 Zoomed view of Response for Case 1 (b) - Rigid supports

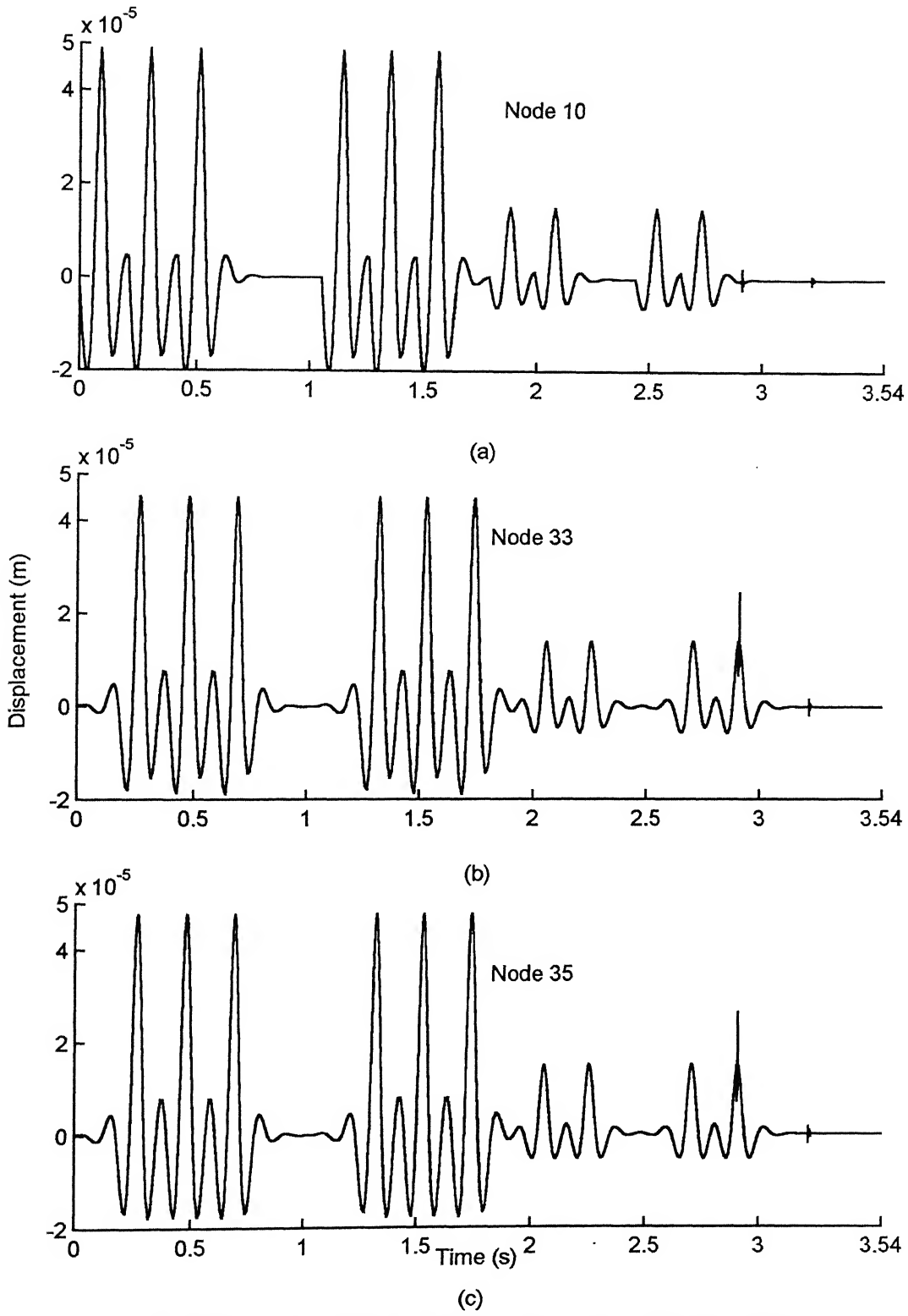

Fig 4.12 Rail Response for Case 2 (b) - Rigid Supports
(a) node 10 , (b) node 33 and (c) node 35

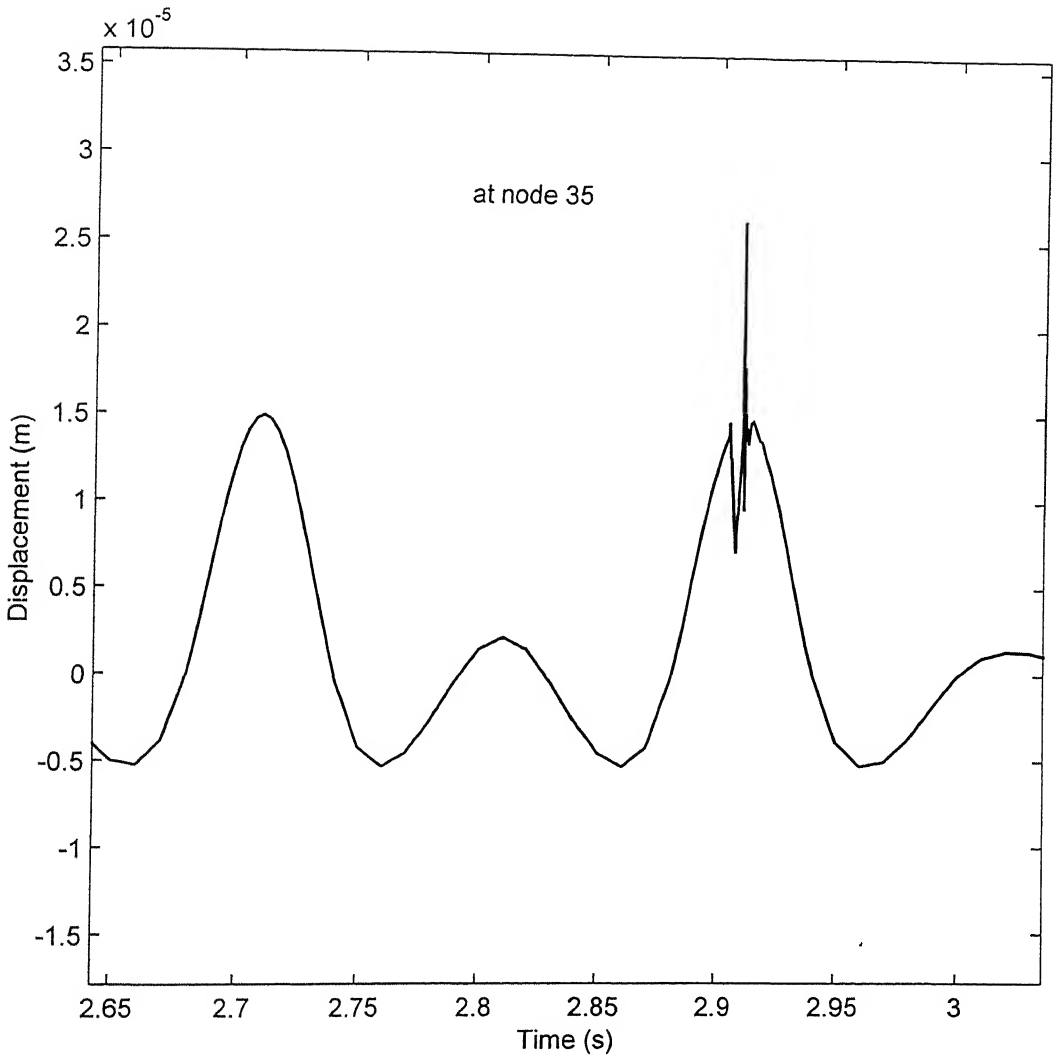

Fig 4.13 Zoomed view of Response for Case 2 (b) - Rigid supports

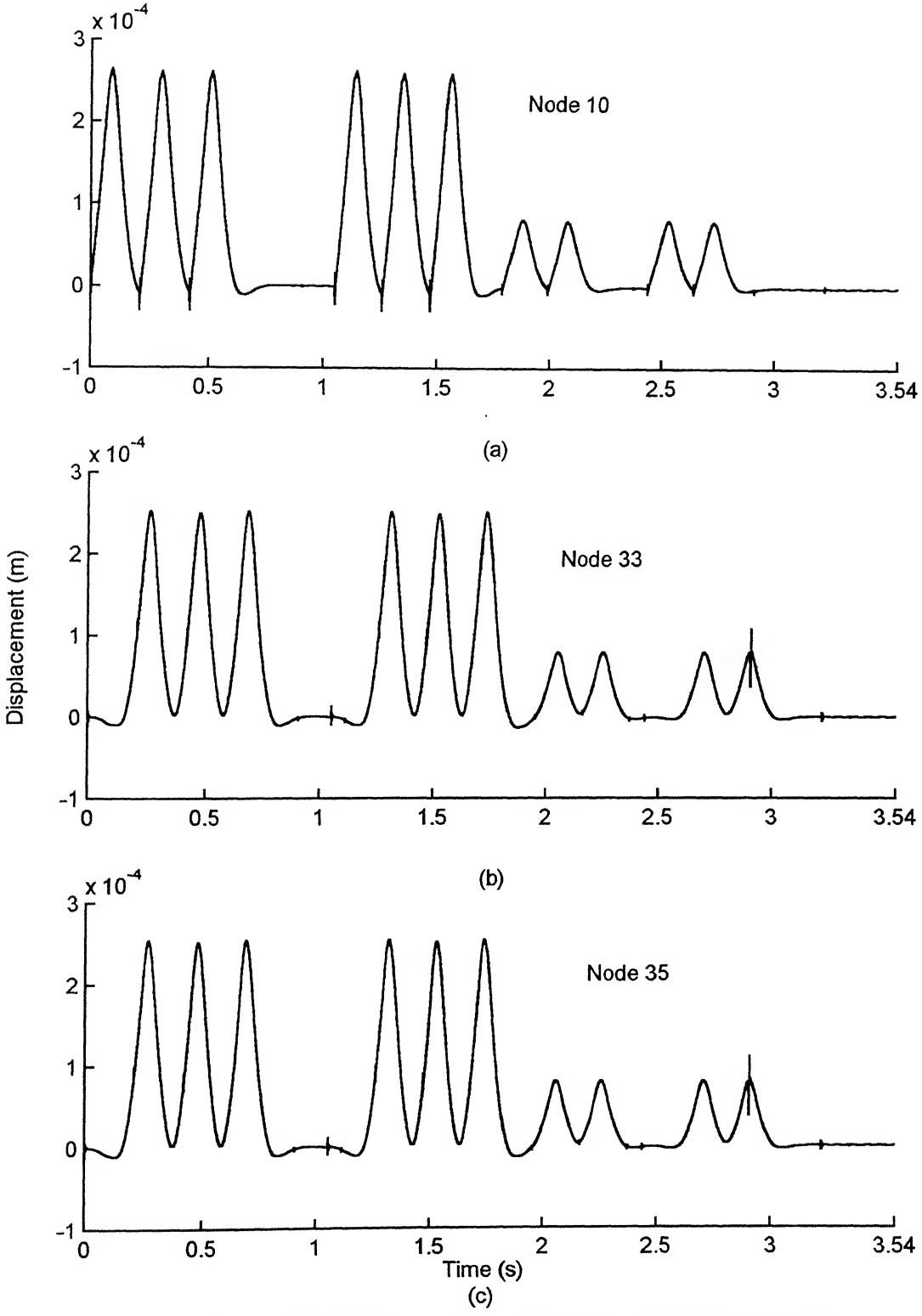

Fig 4.14 Rail Response for Case 2 (b) - Flexible supports
(a) node 10, (b) node 33 and (c) node 35

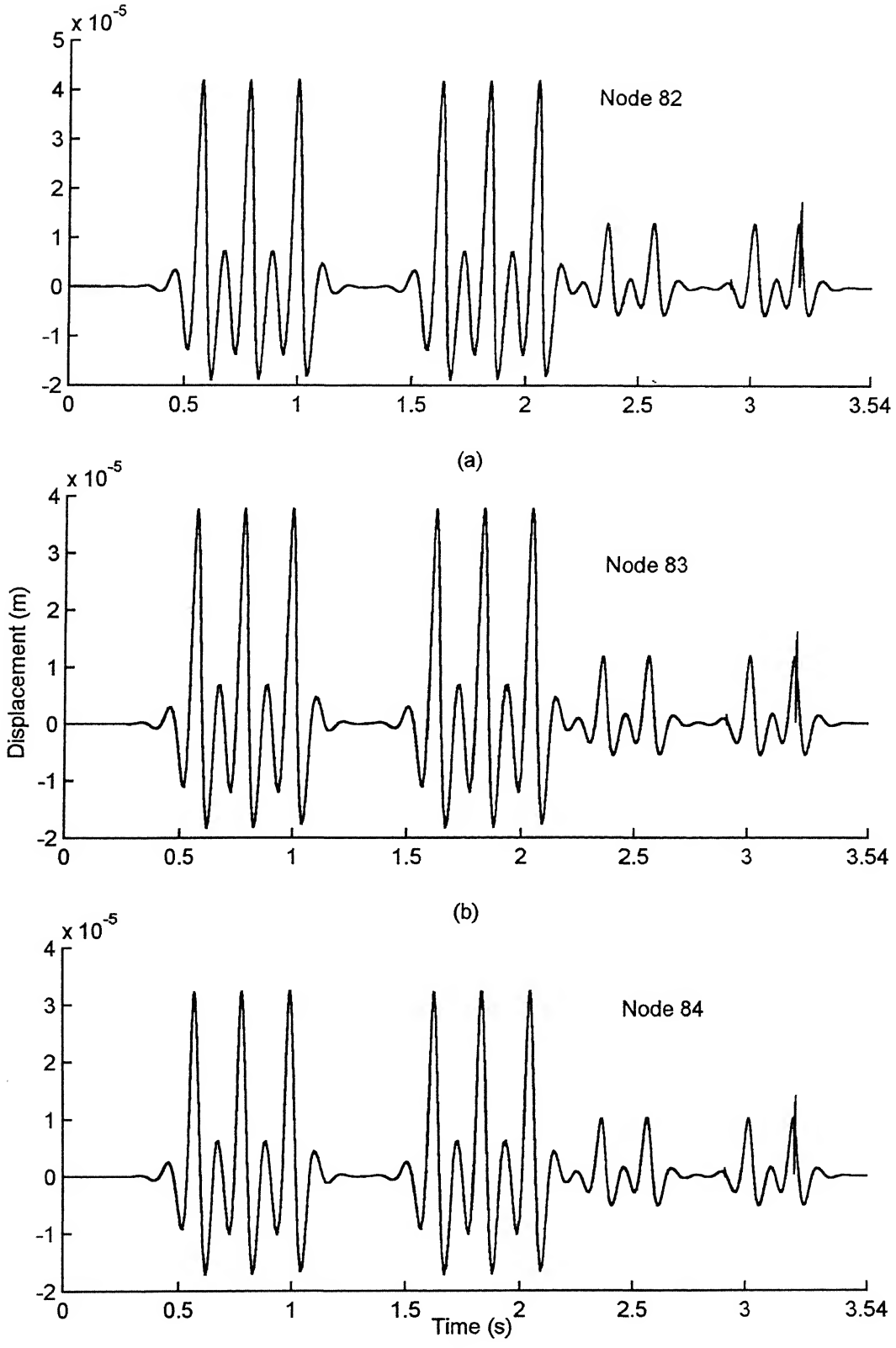

Fig 4.15 Rail Response for Case 2 (b) - Rigid supports

(a) node 82, (b) node 83 and (c) node 84

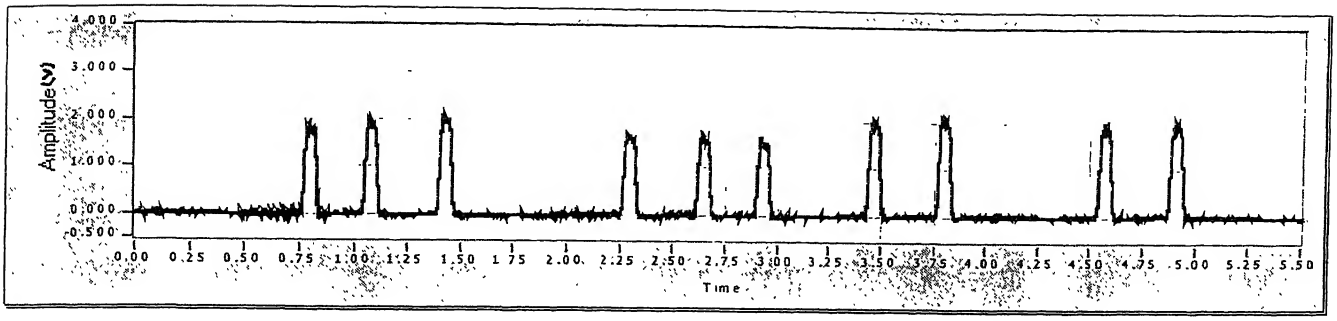

(a) NORMAL WHEELS

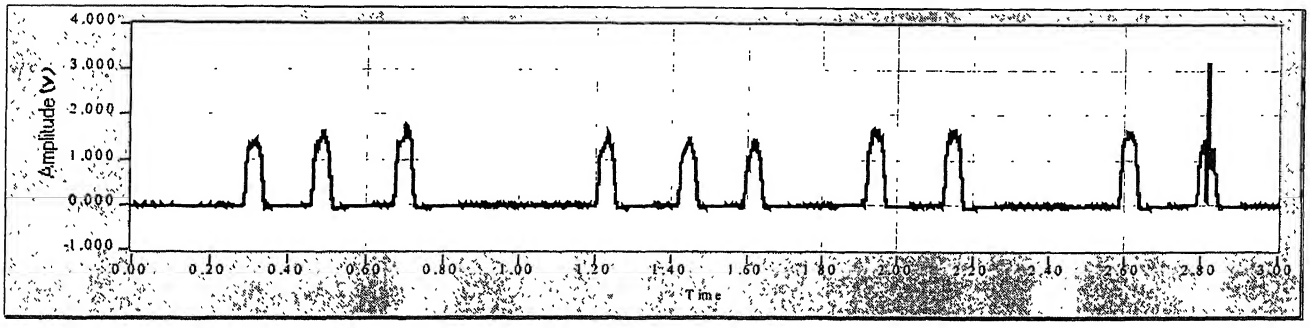

(b) NORMAL WHEELS WITH A FLAT WHEEL (10th Number)

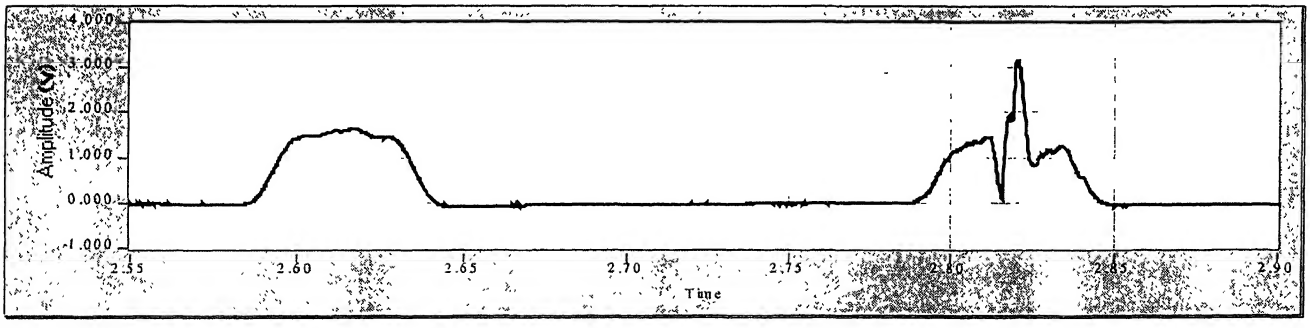

(c) ZOOMED VIEW OF A FLAT WHEEL WITH NORMAL WHEEL

Fig 4.16 Strain gauge Response obtained at test site

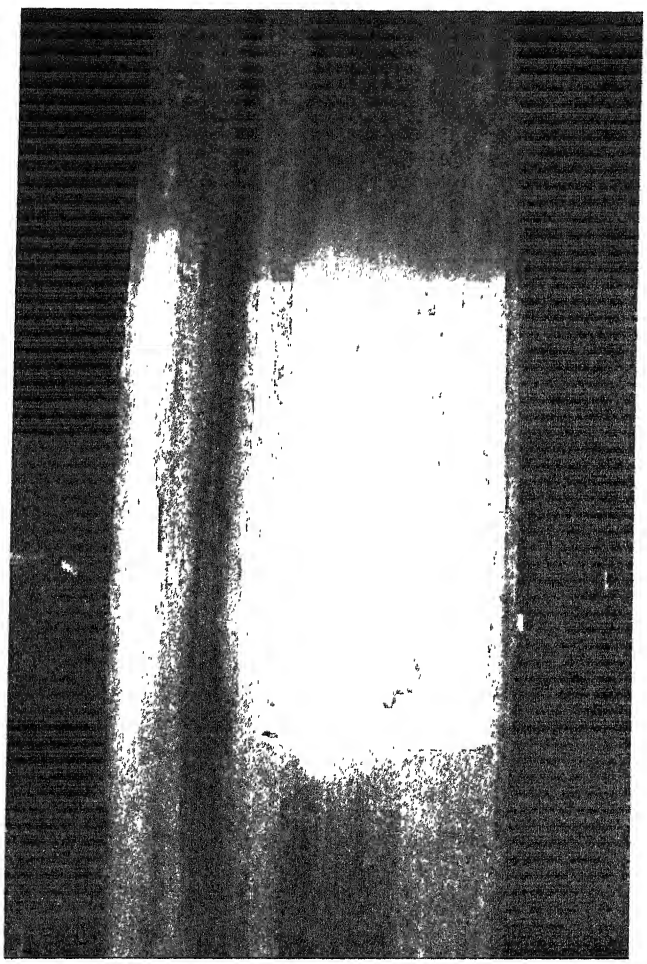

Fig 4.17 Typical flat on a wheel

CHAPTER 5

CONCLUSIONS

A finite element model has been developed during the present work to describe the rail dynamics under a moving train. The model can incorporate train wheels with flats. The wheel flat has been modeled as a 'lift-hit' phenomenon. The rail is taken to be multi-span continuous beam and is modeled through 2-D beam elements. Natural frequencies and mode shapes are obtained and the results are validated by comparison with results obtained through analytical formulations. The train is modeled through multiple moving loads. The model is found to correctly represent the experimentally observed test patterns. Comparison of response patterns due to normal wheel loading and wheel-flat loading has been made. Distinct features have been found in the response patterns, which can aid in development of algorithms for wheel-flat detection. Displacement response is found to provide better information on the presence or absence of flatness in wheels. The acceleration plots appear to contain a large number of frequency components and need to be analyzed more rigorously, than done in the present work, for extraction of meaning information.

The present work is restricted to a single flat on a single wheel on the train. The model developed during the present study can be readily employed to carry out further investigations on the rail response under the influence of multiple flats on the same wheel. Response under wheel-flats on more than one wheel also needs to be investigated. Such a study will help in designing better flat detection algorithms. Further work also needs to be carried out study the influence of various rail parameters like sleeper distance, stiffness and damping on the vibration magnitudes.

REFERENCES

1 Stokes, Sir G. G., "Discussion of a Differential Equation Relating to Breaking of Railway Bridges", *Mathematics Physics Paper*, Vol. 2, p. 179, 1849.

2 Timoshenko, S. P., "On the Forced Vibration of Bridges", *Philosophical Magazine*, Vol. 43, p. 1018, 1922.

3 Lowan, A. N., "On Transverse Oscillations of Beams Under the Action of Moving Variable Loads", *Philosophical Magazine*, Vol. 19,series 7, p.708, 1935.

4 Ayre, R.S., Ford George and Jacobsen, L.S., "Transverse Vibration of a Two Span Beam Under Action of a Moving Constant Force", *Journal of Applied Mechanics*, Vol. 17, p. 1 - 12, 1950.

5 Timoshenko, S. P., "*Vibration Problems in Engineering*", D. Van Nostrand Company, Inc., New York, 1955.

6 Cai, C. W., Cheung, Y .K., and Chan, H. C., "Dynamic Response of Infinite Continuous Beams Subjected to a Moving Force", *Journal of Sound and Vibration*, Vol. 123, p. 461 - 472, 1988.

7 Nielsen, J. C. O. and Igelend, A., "Vertical Dynamic Interaction Between Train and Track - Influence of Wheel and Track Imperfections," *Journal of Sound and Vibration*, Vol. 187, p. 825 - 839, 1995.

8 Thambiratnam, D. and Zhuge, Y., "Dynamic Analysis of Beams on an Elastic Foundation subjected to Moving Loads," *Journal of sound and vibration,* Vol. 198, p. 149 - 169, 1996.

9 Abu Hilal, M. and Zibdeh, H. S., "Vibration Analysis of Beams with General Boundary Conditions Traversed by a Moving Force," *Journal of Sound and Vibration*, Vol. 229, p. 377 - 388, 2000.

10 Jong-shyong Wu and Po-Yun Shih, "Dynamic Response of Railway and Carriage Under the High-speed Moving loads," *Journal of Sound and Vibration*, Vol. 236, p. 61 - 87, 2000.

11 Wu, T. X. and Thompson, D.J., "Vibration Analysis of Railway Track with Multiple wheels on the Rail,' *Journal of Sound and Vibration*, Vol. 239, p. 69 - 97, 2001